

Uncertainty-Aware Bayes' Rule and Its Applications

Shixiong Wang* 

Abstract. Bayes' rule has enabled innumerable powerful algorithms of statistical signal processing and statistical machine learning. However, when model misspecifications exist in prior and/or data distributions, the direct application of Bayes' rule is questionable. Philosophically, the key is to balance the relative importance between prior and data distributions when calculating posterior distributions: if prior distributions are overly conservative (i.e., exceedingly spread), we upweight the prior belief; if prior distributions are overly opportunistic (i.e., exceedingly concentrated), we downweight the prior belief. The same operation also applies to data distributions. This paper studies a generalized Bayes' rule, called uncertainty-aware Bayes' rule, to technically realize the above philosophy, thus combating the model uncertainties in prior and/or data distributions. Applications of the uncertainty-aware Bayes' rule on classification and estimation are discussed: In particular, the uncertainty-aware Bayes classifier, the uncertainty-aware Kalman filter, the uncertainty-aware particle filter, and the uncertainty-aware interactive-multiple-model filter are suggested and experimentally validated.

MSC2020 subject classifications: Primary 62F15, 62F35; secondary 62P30, 68T37.

Keywords: Bayes' Rule, Uncertainty Awareness, Entropy Method, Signal Processing, Machine Learning.

1 Introduction

Bayes' rule has countless successful applications in statistical signal processing and statistical machine learning such as Kalman filter, particle filter, Bayesian hypothesis testing, naive Bayes classifier, Bayesian optimization, Bayesian bandits, and Bayesian networks. Consider a data-generating distribution $p_{\theta_0}(\mathbf{y})$ parametrized by unknown $\theta_0 \in \Theta \subseteq \mathbb{R}^d$ where Θ is the parameter space. We aim to estimate the true value θ_0 using n collected samples $\{\mathbf{y}_1, \mathbf{y}_2, \dots, \mathbf{y}_n\} \subset \mathcal{Y}$ from $p_{\theta_0}(\mathbf{y})$ where $\mathcal{Y} \subseteq \mathbb{R}^l$ is the domain of p_{θ_0} . Bayes' rule

$$p(\boldsymbol{\theta}|\mathbf{y}) \propto p(\boldsymbol{\theta}) \cdot p(\mathbf{y}|\boldsymbol{\theta}), \quad \forall \mathbf{y} \in \mathcal{Y}, \forall \boldsymbol{\theta} \in \Theta \quad (1)$$

suggests the law of calculating the posterior distribution $p(\boldsymbol{\theta}|\mathbf{y})$ after observing the sample \mathbf{y} using the likelihood function $\boldsymbol{\theta} \mapsto p(\mathbf{y}|\boldsymbol{\theta}) := p_{\boldsymbol{\theta}}(\mathbf{y})$ and the prior distribution $p(\boldsymbol{\theta})$. Conceptually, the prior distribution $p(\boldsymbol{\theta})$ encodes our prior belief that $\boldsymbol{\theta} \in \Theta$ is the true value and the likelihood function $p(\mathbf{y}|\boldsymbol{\theta})$ indicates our \mathbf{y} -data evidence that $\boldsymbol{\theta}$ is the true value. Hence, the posterior distribution $p(\boldsymbol{\theta}|\mathbf{y})$ denotes our integrated posterior

arXiv: 2311.05532

*Institute of Data Science, National University of Singapore, Singapore, and Department of Electrical and Electronic Engineering, Imperial College London, United Kingdom, s.wang@u.nus.edu.

belief that $\boldsymbol{\theta}$ is the true value. For a review of Bayes' rule, see [van de Schoot et al. \(2021\)](#).

From the optimization-centric perspective, the Bayesian posterior (1) solves the following problem

$$p(\boldsymbol{\theta}|\mathbf{y}) = \underset{q(\boldsymbol{\theta})}{\operatorname{argmin}} \mathbb{E}_{\boldsymbol{\theta} \sim q(\boldsymbol{\theta})} [-\ln p(\mathbf{y}|\boldsymbol{\theta})] + \operatorname{KL} [q(\boldsymbol{\theta}) \| p(\boldsymbol{\theta})], \quad (2)$$

where $\operatorname{KL} [q(\boldsymbol{\theta}) \| p(\boldsymbol{\theta})]$ denotes the Kullback–Leibler (KL) divergence of $q(\boldsymbol{\theta})$ from $p(\boldsymbol{\theta})$; see, e.g., [Blei et al. \(2017\)](#); [Knoblauch et al. \(2022\)](#) for technical details. This perspective intuitively supports the validity of the Bayesian posterior (1): it maximizes the \mathbf{y} -data evidence conveyed in $p(\mathbf{y}|\boldsymbol{\theta})$ and simultaneously minimizes the deviation from the prior belief $p(\boldsymbol{\theta})$.

In using the conventional Bayes' rule (1), the fundamental assumption is that the data distribution $\mathbf{y} \mapsto p(\mathbf{y}|\boldsymbol{\theta})$ for every $\boldsymbol{\theta} \in \Theta$ and the prior distribution $p(\boldsymbol{\theta})$ are accurate: that is, $p(\boldsymbol{\theta})$ is indeed our best prior knowledge about the true value $\boldsymbol{\theta}_0$ and the data $\{\mathbf{y}_1, \mathbf{y}_2, \dots, \mathbf{y}_n\}$ are indeed sampled from $p_{\boldsymbol{\theta}_0}(\mathbf{y})$. However, this assumption is highly untenable in practice, and as a result, the performance of algorithms relying on the conventional Bayesian posterior (1) significantly degrades ([Huber and Ronchetti, 2009](#), Chap. 15), ([Knoblauch et al., 2022](#)). For specific examples and illustrations from the general Bayesian statistics community, see, e.g., [Berger \(1994\)](#); [Insua and Ruggeri \(2000\)](#); [Ruggeri et al. \(2005\)](#); [Gelman et al. \(2013\)](#); [Medina et al. \(2022\)](#); for those from the Bayesian statistical signal processing community, see, e.g., [Petersen and Savkin \(1999\)](#); [Zoubir et al. \(2018\)](#); [Shmaliy et al. \(2018\)](#); [Wang \(2022a\)](#).

Facing the model uncertainties before applying Bayes' rule, one way is to improve the modeling accuracy and reduce such uncertainties whenever new domain knowledge arrives, for example, by replacing Gaussian distributions with Student's t distributions when outliers exist ([Gelman et al., 2013](#), Chap. 17); approaches in line with this principle are frequently referred to as adaptive methods. When improving the modeling accuracy is practically challenging due to, e.g., limited domain knowledge, the other way that tolerates or withstands the model uncertainties can be attractive to practitioners; methods aligning with this principle are called robust methods. According to [Huber and Ronchetti \(2009](#), Sec. 15.2), the robust design can be achieved by two operations: a) adjusting the prior distribution (i.e., prior belief) and/or the data distribution (i.e., data evidence); or b) balancing the relative importance between them. The boundary between the two operations, however, is not sharp because to make one distribution noninformative (e.g., to widen its spread on Θ) is to downweight its relative importance, compared to the other, in calculating the posterior; cf. (1). Four technical approaches that realize the above philosophy of Bayesian robustness include the following.

- A1) Employing noninformative priors (e.g., uniform or large-entropy distributions) to admit the lack of prior knowledge ([Berger, 1994](#)). In this case, the data distribution $p(\mathbf{y}|\boldsymbol{\theta})$ is assumed to be accurate and the Bayes' rule (1) calculating the posterior remains unchanged.

- A2) Modifying the data distribution to better accommodate data evidence under the likelihood uncertainty (Nguyen et al., 2019), (Huber and Ronchetti, 2009, Chaps. 4 and 5). For a given $\boldsymbol{\theta}$, this amounts to adjusting its \mathbf{y} -data evidence $p(\mathbf{y}|\boldsymbol{\theta})$. In this case, the prior distribution $p(\boldsymbol{\theta})$ is assumed to be accurate and the rule generating the posterior stays the same as (1).
- A3) Leveraging the maximum entropy scheme to adjust, and therefore balance the relative importance between, the prior distribution $p(\boldsymbol{\theta})$ and the data distribution $p(\mathbf{y}|\boldsymbol{\theta})$ (Wang, 2022b). To be specific, if the prior distribution $p(\boldsymbol{\theta})$ is uncertain, we replace it with the maximum entropy distribution within its neighbor (e.g., a distributional ball), thus downweighting the impact of the prior belief on the posterior distribution. That is, in calculating the posterior distribution using (1), the prior distribution $p(\boldsymbol{\theta})$ is replaced with the following maximum entropy distribution $f^*(\boldsymbol{\theta})$:

$$\begin{aligned} f^*(\boldsymbol{\theta}) = \operatorname{argmax}_{f(\boldsymbol{\theta})} & \int_{\Theta} -f(\boldsymbol{\theta}) \ln f(\boldsymbol{\theta}) d\boldsymbol{\theta} \\ \text{s.t.} & \begin{cases} S(f(\boldsymbol{\theta}), p(\boldsymbol{\theta})) \leq \epsilon \\ \int_{\Theta} f(\boldsymbol{\theta}) d\boldsymbol{\theta} = 1. \end{cases} \end{aligned} \quad (3)$$

where $S(f(\boldsymbol{\theta}), p(\boldsymbol{\theta}))$ defines a similarity measure between two distributions $f(\boldsymbol{\theta})$ and $p(\boldsymbol{\theta})$, and $\epsilon \geq 0$ is the uncertainty quantification level of $p(\boldsymbol{\theta})$. The larger the radius ϵ is, the larger the entropy of $f^*(\boldsymbol{\theta})$ is, and therefore, the more uniformly $f^*(\boldsymbol{\theta})$ spreads on Θ and the more the prior distribution $p(\boldsymbol{\theta})$ is downweighted. The same operation applies to the data distribution $p(\mathbf{y}|\boldsymbol{\theta})$ for every $\boldsymbol{\theta}$, if it is uncertain, to reduce the impact of the data distribution on the posterior distribution. As a result, the relative importance of the prior distribution and the data distribution is determined by their corresponding uncertainty radii. Note that, in this case, the Bayes' rule (1) is not altered as well.

- A4) Modifying the Bayes' rule (1). One trending and computationally efficient representative in this category is the α -posterior by introducing a nonnegative parameter α in calculating the posterior (Alquier and Ridgway, 2020; Medina et al., 2022), (Ghosal and Van der Vaart, 2017, Sec. 6.8.5 and Sec. 8)

$$p_{\alpha}(\boldsymbol{\theta}|\mathbf{y}) \propto p(\boldsymbol{\theta}) \cdot p^{\alpha}(\mathbf{y}|\boldsymbol{\theta}), \quad \alpha \geq 0, \quad (4)$$

which solves an α -weighted version of (2), i.e.,

$$p_{\alpha}(\boldsymbol{\theta}|\mathbf{y}) = \operatorname{argmin}_{q(\boldsymbol{\theta})} \alpha \cdot \mathbb{E}_{\boldsymbol{\theta} \sim q(\boldsymbol{\theta})} [-\ln p(\mathbf{y}|\boldsymbol{\theta})] + \text{KL}[q(\boldsymbol{\theta}) \| p(\boldsymbol{\theta})], \quad \alpha \geq 0. \quad (5)$$

Through the above formula, the prior distribution is assumed to be accurate and the importance of the data distribution is reduced if $0 \leq \alpha < 1$, remains unchanged if $\alpha = 1$, and is increased if $\alpha > 1$. Other generalizations to (2) propose to replace the negative logarithm cost function $-\ln p(\mathbf{y}|\boldsymbol{\theta})$ with a general user-designed version $h: \mathcal{Y} \times \Theta \rightarrow \mathbb{R}_+$, and/or substitute the Kullback–Leibler divergence with other user-specified divergences D such as the Rényi divergence (Knoblauch et al., 2022, Table 1), giving rise to the Rule-of-Three framework (Knoblauch et al., 2022)

$$\min_{q(\boldsymbol{\theta})} \mathbb{E}_{\boldsymbol{\theta} \sim q(\boldsymbol{\theta})} [h(\mathbf{y}, \boldsymbol{\theta})] + D[q(\boldsymbol{\theta}) \| p(\boldsymbol{\theta})]. \quad (6)$$

Note that (6) encompasses (5) as a special case. The α -posterior (4) is well-believed to be robust against the misspecified likelihood function (i.e., data distribution) (Wu and Martin, 2023; Medina et al., 2022), while the posteriors under the Rule-of-Three (6) can combat uncertainties in both the prior distribution and the data distribution (Knoblauch et al., 2022).

Despite the remarkable capabilities of the existing approaches in addressing uncertainties in both the prior distribution and the data distribution, two issues naturally arise:

- I1) The α -posterior, although computationally attractive due to its closed-form feature, is not reliable in addressing uncertainties in the prior distribution (Knoblauch et al., 2022). To be specific, if $\alpha > 1$, the α -posterior tends to be robust against the uncertainties in the prior distribution because the prior belief is downweighted relative to the data distribution, but the α -posterior simultaneously tends to concentrate on the maximum-likelihood point estimate. This concentration property reduces the spread of the posterior distribution so that the posterior distribution has no sufficient ability for uncertainty quantification, i.e., the ability to cover the true parameter θ_0 with high probability; see Wu and Martin (2023). In contrast, if $0 \leq \alpha < 1$, the posterior's over-concentration can be avoided, but at the expense of not being robust against the uncertainties in the prior distribution. For detailed justifications on the deficiency of the α -posterior, see Knoblauch et al. (2022, Appendix B.3.1). For a motivational example, see below.

Example 1 (Deficiency of α -Posterior). Suppose the true data-generating distribution is a one-dimensional unit-variance Gaussian density $\mathcal{N}(y; 0, 1)$, that is, $\theta_0 = 0$. At measurement $y = 0.1$, the data evidence of θ (i.e., normalized likelihood function) is $l_{y=0.1}(\theta) = \mathcal{N}(\theta; 0.1, 1)$. If we adopt the prior distribution to be $p(\theta) := \mathcal{N}(\theta; 1, 1)$, then $p(\theta)$ is an unreliable prior because $p(\theta)$ is significantly biased. In this case, a good strategy to downweight the misleading information in the prior is to let the prior $p(\theta)$ be noninformative by inflating its variance, that is, $p(\theta) := \mathcal{N}(\theta; 1, 1/\beta)$ where $0 < \beta < 1$. As a result, the corresponding posterior would be $\mathcal{N}(\theta; \frac{0.1+\beta}{1+\beta}, \frac{1}{1+\beta})$. By using a small value for β (e.g., 0.01), the posterior bias $\frac{0.1+\beta}{1+\beta}$ can be greatly reduced without overly concentrating the posterior. In contrast, if the α -posterior is used, the corresponding posterior would be $\mathcal{N}(\theta; \frac{1+0.1\alpha}{1+\alpha}, \frac{1}{1+\alpha})$, which implies that reducing the posterior bias $\frac{1+0.1\alpha}{1+\alpha}$ by $\alpha > 1$ also largely concentrates the posterior. \square

- I2) The maximum entropy scheme and the Rule-of-Three framework, although capable of handling uncertainties in both the prior distribution and the data distribution, tend to be computationally prohibitive in real-time data analytics, such as signal processing, because the existence of closed-form solutions is not necessarily guaranteed when complex discrepancy measures for distributions are used; recall S in (3) and D in (6). As a result, sufficient computational resources must be employed to accommodate numerical methods, which excludes the applicability of these uncertainty-aware methods in computation-limited scenarios, e.g., low-cost embedded processors.

To address the two issues above, this paper proposes a new optimization-centric interpretation of the Bayes' rule, differently from (2), and formulates a new framework for generating uncertainty-aware posteriors.

- **New Optimization-Centric Interpretation:** By introducing the concept of *likelihood distribution* $l_{\mathbf{y}}(\boldsymbol{\theta}) := \frac{p(\mathbf{y}|\boldsymbol{\theta})}{\int p(\mathbf{y}|\boldsymbol{\theta})d\boldsymbol{\theta}}$, which is a \mathbf{y} -parametric distribution of $\boldsymbol{\theta}$, we show that the Bayesian posterior (1) solves the following optimization problem

$$p(\boldsymbol{\theta}|\mathbf{y}) = \underset{q(\boldsymbol{\theta})}{\operatorname{argmin}} \operatorname{KL} [q(\boldsymbol{\theta}) \| p(\boldsymbol{\theta})] + \operatorname{KL} [q(\boldsymbol{\theta}) \| l_{\mathbf{y}}(\boldsymbol{\theta})] + \operatorname{Ent} q(\boldsymbol{\theta}), \quad (7)$$

where $\operatorname{Ent} q(\boldsymbol{\theta}) := -\int q(\boldsymbol{\theta}) \ln q(\boldsymbol{\theta}) d\boldsymbol{\theta}$ denotes the differential entropy of $q(\boldsymbol{\theta})$; see Definition 1 and Lemma 1. Model (7) reveals that the posterior distribution $p(\boldsymbol{\theta}|\mathbf{y})$ is a minimum-entropy (i.e., minimum spread) distribution that is simultaneously close to the prior belief $p(\boldsymbol{\theta})$ and the \mathbf{y} -data evidence $l_{\mathbf{y}}(\boldsymbol{\theta})$; NB: the evidence from the data \mathbf{y} is encoded in the distribution $l_{\mathbf{y}}(\boldsymbol{\theta})$. We notice that the new interpretation (7) links the Bayesian inference problem to the probability density fusion problem (Koliander et al., 2022). To be specific, in Bayesian inference, the posterior distribution $p(\boldsymbol{\theta}|\mathbf{y})$ is an entropy-regularized KL-barycenter of the prior distribution $p(\boldsymbol{\theta})$ and the likelihood distribution $l_{\mathbf{y}}(\boldsymbol{\theta})$, while in probability density fusion, there is no entropy-regularizer presented when computing the KL-barycenter of different distributions.

- **New Uncertainty-Aware Framework:** Aligning with the philosophy of Bayesian robustness discussed before (i.e., to balance the relative importance between $p(\boldsymbol{\theta})$ and $l_{\mathbf{y}}(\boldsymbol{\theta})$ and to control the spread of the resultant posterior distribution), motivated by (7), this paper proposes to study the following optimization problem

$$\min_{q(\boldsymbol{\theta})} \alpha_1 \operatorname{KL} [q(\boldsymbol{\theta}) \| p(\boldsymbol{\theta})] + \alpha_2 \operatorname{KL} [q(\boldsymbol{\theta}) \| l_{\mathbf{y}}(\boldsymbol{\theta})] + \alpha_3 \operatorname{Ent} q(\boldsymbol{\theta}), \quad (8)$$

where α_1 , α_2 , and α_3 are weights to emphasize or discount the corresponding terms, respectively; the weights can be negative to let the posterior be away from $p(\boldsymbol{\theta})$ or $l_{\mathbf{y}}(\boldsymbol{\theta})$, or to let the posterior entail large entropy (i.e., large spread). The posterior distribution solving the uncertainty-aware formulation (8) is given by

$$p_g(\boldsymbol{\theta}|\mathbf{y}) \propto p^{\frac{\alpha_1}{\alpha_1 + \alpha_2 - \alpha_3}}(\boldsymbol{\theta}) \cdot l_{\mathbf{y}}^{\frac{\alpha_2}{\alpha_1 + \alpha_2 - \alpha_3}}(\boldsymbol{\theta}), \quad (9)$$

if $\alpha_1 + \alpha_2 > \alpha_3$; see Theorem 1. The existing α -posterior can be recovered by setting $\alpha_1 = 1$ and $\alpha_2 = \alpha_3 = \alpha$. For notational simplicity, we rewrite (9) by employing the parameter pair (α, β) and suggest the uncertainty-aware Bayes' rule in Definition 2:

$$p_g(\boldsymbol{\theta}|\mathbf{y}) \propto p^\beta(\boldsymbol{\theta}) \cdot p^\alpha(\mathbf{y}|\boldsymbol{\theta}), \quad 0 \leq \alpha, \beta < \infty. \quad (10)$$

This paper names the uncertainty-aware (UA) posterior distribution in (10) as the (α, β) -posterior, generalizing the existing α -posterior from a new perspective rather than the scheme (5) and the Rule-of-Three framework (6).

Compared to the α -posterior strategy, the maximum entropy scheme, and the Rule-of-Three framework, the practical benefits of the proposed UA framework (8) and the UA posterior (10) are three-fold:

- The proposed framework (8) can achieve robustness against uncertainties in the prior distribution by using small values of $\alpha_1 \geq 0$ and that in the likelihood distribution by using small values of $\alpha_2 \geq 0$. Simultaneously, the framework can restrict the posterior distribution from over-concentration by using small values of $\alpha_3 \geq 0$. Therefore, when α_1 , α_2 , and α_3 are suitably balanced, Issue I1) faced by the existing α -posterior can be avoided by the (α, β) -posterior (10); NB: α and β are determined by α_1 , α_2 , and α_3 . Intuitively, this benefit comes from the extra freedom introduced by the new parameter β , that is, by **not** forcing $\alpha_2 = \alpha_3$.
- The (α, β) -posterior is as computationally lightweight as the α -posterior. This computational benefit cannot be shared by the existing Rule-of-Three framework under complex cost functions h and divergences D , as well as the existing maximum entropy scheme under complex distributional balls. Therefore, Issue I2) can also be attacked by the (α, β) -posterior.
- In the (α, β) -posterior, the maximum entropy transform in (3) on the prior and data distributions can be achieved by adjusting parameters α and β . To be specific, for example, $p^\beta(\boldsymbol{\theta})$ (after normalization) can have larger or smaller entropy than $p(\boldsymbol{\theta})$; see Corollary 1. Recall that the entropy of a distribution depicts its spread; the more the prior or likelihood distribution spreads, the less influence it has on the posterior.

The uncertainty awareness of the (α, β) -posterior includes two aspects: conservatism (i.e., robustness) and opportunism. When the information (i.e., prior belief or data evidence) is believed to be overly opportunistic (i.e., exceedingly concentrated), we pursue robustness and downweight the information by increasing the spread. Conversely, when the information is believed to be overly conservative (i.e., exceedingly spread), we pursue opportunism and upweight the information by decreasing the spread. Motivated by (7), this paper employs the entropy value of a distribution as the measure of its spread, which is also a convention in probability and statistics. We show that for $\alpha, \beta < 1$, the (α, β) -posterior can reflect the robustness philosophy to downweight the prior belief and/or data evidence, as the maximum entropy scheme does; in contrast, for $\alpha, \beta > 1$, the (α, β) -posterior can reflect the opportunism philosophy and upweight the prior belief and/or data evidence; see Corollary 1. Moreover, we show that the α -scaled distribution $l_{\mathbf{y}}^\alpha(\boldsymbol{\theta})$, after normalization, can be closer in the KL sense to the underlying true data distribution than the original $l_{\mathbf{y}}(\boldsymbol{\theta})$, for some $\alpha \geq 0$; the similar statement applies to β -scaled $p^\beta(\boldsymbol{\theta})$ and $p(\boldsymbol{\theta})$; see Theorem 4. This scaling-for-closeness property complementarily justifies the superiority of the proposed (α, β) -posterior over the conventional Bayes' posterior and the existing α -posterior.

Although the two parameters α and β bring excellent freedom for uncertainty awareness in calculating the posterior distribution, their optimal values cannot be determined in a universal way, especially considering different performance preferences in diverse

real-world applications. To be specific, the theoretical optimality of the parameters relies on the underlying true but unknown data-generating distribution (cf. [Medina et al. \(2022, Lemma 1\)](#), [Wu and Martin \(2023, Section 3\)](#), and [Theorem 4](#)), while the practical optimality depends on the specific applications and the employed empirical performance measures. This dilemma also arises in tuning the coefficient α of the α -posterior (4) ([Medina et al., 2022, p. 26](#)), ([Wu and Martin, 2023](#)), the radii ϵ 's of the maximum entropy scheme (3) ([Wang, 2022b, Section V](#)), the parameters involved in h and D of the Rule-of-Three framework (6) ([Knoblauch et al., 2022, p. 36](#)), and the fusion weights of probability density functions ([Koliander et al., 2022, Section VII](#)). Hence, data-driven empirical tuning methods for α and β are unavoidable to achieve satisfactory performances for specific real-world problems; see [Subsection 2.6](#) for details. Key findings of this paper are as follows:

- In some applications such as Bayesian classification, only the ratio α/β matters, while in others such as Bayesian estimation, α and β independently contribute to performances. Therefore, for the former cases, using the α -posterior is sufficient. However, for the latter ones, the (α, β) -posterior is necessary. For a motivational example, recall [Example 1](#); for technical details, see [Subsection 2.5](#); for experimental justifications, see [Subsection 2.7](#).
- To achieve good empirical performances, α may be either larger or smaller than one. The same observation happens for β as well. In contrast, in the literature of the α -posterior, to establish desired properties, such as posterior consistency, asymptotic normality, and robustness, $\alpha \leq 1$ is required; see, e.g., [Miller and Dunson \(2019\)](#); [Medina et al. \(2022\)](#). Hence, building favored theoretical properties in one aspect does not necessarily benefit real-world performances in other aspects; see [Example 4](#) for motivation. For experimental justifications, see [Subsection 2.7](#).

Notation: Random and deterministic quantities are denoted by upright and italic symbols (e.g., \mathbf{y} and \mathbf{y}), respectively. Let \mathbb{R}^d denote the d -dimensional real space. We use $p_{\mathbf{y}}(\mathbf{y})$ to denote the probability density (resp. mass) function of \mathbf{y} if \mathbf{y} is continuous (resp. discrete); when it is clear from the contexts, $p(\mathbf{y})$ is used as a shorthand for $p_{\mathbf{y}}(\mathbf{y})$. The multivariate Gaussian distribution with mean $\boldsymbol{\mu}$ and covariance $\boldsymbol{\Sigma}$ is denoted as $\mathcal{N}(\boldsymbol{\mu}, \boldsymbol{\Sigma})$ and its density function as $\mathcal{N}(\cdot; \boldsymbol{\mu}, \boldsymbol{\Sigma})$. Let $[r] := \{1, 2, \dots, r\}$ be the running index set induced by integer r .

2 Main Results

This paper assumes that (probability) density functions exist (with respect to the Lebesgue measure). To reduce the presentation length, the main results are only given under probability density functions; for probability mass functions, one may just change integrals to sums. To reduce notational clutter, we implicitly mean $\mathbf{y} \in \mathcal{Y}$ and $\boldsymbol{\theta} \in \Theta$ throughout the paper, unless otherwise stated.

2.1 Generalized Bayes' Rule

We begin with the concept of likelihood distribution.

Definition 1 (Likelihood Distribution). Let

$$l_{\mathbf{y}}(\boldsymbol{\theta}) := \frac{p(\mathbf{y}|\boldsymbol{\theta})}{\int_{\Theta} p(\mathbf{y}|\boldsymbol{\theta})d\boldsymbol{\theta}}, \quad \forall \mathbf{y} \quad (11)$$

define the *likelihood distribution* of $\boldsymbol{\theta}$ induced by the likelihood function $\boldsymbol{\theta} \mapsto p(\mathbf{y}|\boldsymbol{\theta})$ evaluated at the sample \mathbf{y} . \square

The integral $\int_{\Theta} p(\mathbf{y}|\boldsymbol{\theta})d\boldsymbol{\theta}$ is well-defined if, for example, Θ is compact and $p(\mathbf{y}|\boldsymbol{\theta})$ is continuous (or bounded and measurable) in $\boldsymbol{\theta}$ on Θ . In practice, requiring the compactness of Θ is not restrictive: 1) for example, the mean and variance of a Gaussian distribution are finite; 2) for another example, the degree of freedom of a Student's t distribution is finite (otherwise, it degenerates to a Gaussian distribution); 3) for a third example, the location and scale parameters of a Cauchy distribution are finite. The likelihood distribution $l_{\mathbf{y}}(\boldsymbol{\theta})$ is a \mathbf{y} -parametric distribution of $\boldsymbol{\theta}$. A direct result of Definition 1 is that the posterior distribution $p(\boldsymbol{\theta}|\mathbf{y})$ given by the conventional Bayes' rule (1) can be expressed as

$$p(\boldsymbol{\theta}|\mathbf{y}) \propto p(\boldsymbol{\theta}) \cdot l_{\mathbf{y}}(\boldsymbol{\theta}). \quad (12)$$

Hereafter, when it is clear from the contexts, we suppress the notational dependence on \mathbf{y} and use $l(\boldsymbol{\theta})$ as a shorthand for $l_{\mathbf{y}}(\boldsymbol{\theta})$. The lemma below gives an interpretation of the origin of the Bayes' rule (12).

Lemma 1 (Conventional Bayes' Rule). *The posterior distribution $p(\boldsymbol{\theta}|\mathbf{y})$ given by the Bayes' rule (1) [or (12)] solves*

$$\min_{q(\boldsymbol{\theta})} \text{KL} [q(\boldsymbol{\theta}) \| p(\boldsymbol{\theta})] + \text{KL} [q(\boldsymbol{\theta}) \| l(\boldsymbol{\theta})] + \text{Ent} q(\boldsymbol{\theta}). \quad (13)$$

Proof. See Appendix A in supplementary materials. \square

Lemma 1 indicates that the posterior distribution $p(\boldsymbol{\theta}|\mathbf{y})$ is an entropy-regularized equal-weight KL-barycenter of the prior distribution $p(\boldsymbol{\theta})$ and the likelihood distribution $l(\boldsymbol{\theta})$; intuitively, $p(\boldsymbol{\theta}|\mathbf{y})$ is a minimum-entropy distribution that is simultaneously close to both the prior distribution (i.e., prior belief) and the likelihood distribution (i.e., \mathbf{y} -data evidence).

Aligning with the philosophy of Bayesian robustness discussed before (i.e., to balance the relative importance between $p(\boldsymbol{\theta})$ and $l(\boldsymbol{\theta})$ and to control the spread of the resultant posterior distribution), we generalize the optimization problem (13) to

$$\min_{q(\boldsymbol{\theta})} \alpha_1 \text{KL} [q(\boldsymbol{\theta}) \| p(\boldsymbol{\theta})] + \alpha_2 \text{KL} [q(\boldsymbol{\theta}) \| l(\boldsymbol{\theta})] + \alpha_3 \text{Ent} q(\boldsymbol{\theta}), \quad (14)$$

where α_1 , α_2 , and α_3 are weights. To let $q(\boldsymbol{\theta})$ be close to $p(\boldsymbol{\theta})$ and $l(\boldsymbol{\theta})$, without loss of practicality, the following assumption is imposed.

Assumption 1. We assume that $0 \leq \alpha_1 < \infty$, $0 \leq \alpha_2 < \infty$, and $-\infty < \alpha_3 < \infty$. \square

Depending on whether to pursue the maximum or minimum entropy of $q(\boldsymbol{\theta})$, α_3 can take any finite value on the whole real line \mathbb{R} . We term the distribution solving the generalized problem (14) the *generalized Bayesian posterior distribution*.

Theorem 1 (Generalized Bayes' Rule). *The generalized posterior distribution $p_g(\boldsymbol{\theta}|\mathbf{y})$ solving (14) is given by*

$$p_g(\boldsymbol{\theta}|\mathbf{y}) \propto p^{\frac{\alpha_1}{\alpha_1+\alpha_2-\alpha_3}}(\boldsymbol{\theta}) \cdot l^{\frac{\alpha_2}{\alpha_1+\alpha_2-\alpha_3}}(\boldsymbol{\theta}), \quad (15)$$

or equivalently,

$$p_g(\boldsymbol{\theta}|\mathbf{y}) \propto p^{\frac{\alpha_1}{\alpha_1+\alpha_2-\alpha_3}}(\boldsymbol{\theta}) \cdot p^{\frac{\alpha_2}{\alpha_1+\alpha_2-\alpha_3}}(\mathbf{y}|\boldsymbol{\theta}), \quad (16)$$

when $\alpha_3 < \alpha_1 + \alpha_2$, provided that the right-hand-side terms are integrable on Θ . When $\alpha_3 = \alpha_1 + \alpha_2$, $p_g(\boldsymbol{\theta}|\mathbf{y})$ is an arbitrary distribution supported on the set Θ^* where $\Theta^* := \operatorname{argmax}_{\boldsymbol{\theta}} \alpha_1 \ln p(\boldsymbol{\theta}) + \alpha_2 \ln l(\boldsymbol{\theta})$ contains all weighted maximum a-posteriori estimates.

Proof. See Appendix B in supplementary materials. \square

In Theorem 1 and throughout this paper, we only consider the case where $\alpha_3 \leq \alpha_1 + \alpha_2$ for technical simplicity; see the proof of Theorem 1 for details. By rewriting the generalized posterior distribution in (15) for notational simplicity, we introduce the (α, β) -posterior.

Definition 2 ((α, β) -Posterior). The (α, β) -posterior induced by the prior distribution $p(\boldsymbol{\theta})$ and the likelihood distribution $l(\boldsymbol{\theta})$ is defined as

$$p_g(\boldsymbol{\theta}|\mathbf{y}) \propto p^\beta(\boldsymbol{\theta}) \cdot l^\alpha(\boldsymbol{\theta}), \quad (17)$$

where $0 \leq \alpha, \beta < \infty$, if the right-hand-side term is integrable on Θ . When α and β are infinity, the (α, β) -posterior $p_g(\boldsymbol{\theta}|\mathbf{y})$ is defined as an arbitrary distribution supported on Θ^* where $\Theta^* := \operatorname{argmax}_{\boldsymbol{\theta}} \alpha_1 \ln p(\boldsymbol{\theta}) + \alpha_2 \ln l(\boldsymbol{\theta})$. \square

Note that, compared with (15), $\beta := \frac{\alpha_1}{\alpha_1+\alpha_2-\alpha_3} \in [0, \infty)$ and $\alpha := \frac{\alpha_2}{\alpha_1+\alpha_2-\alpha_3} \in [0, \infty)$, if $\alpha_3 < \alpha_1 + \alpha_2$. When $\alpha_3 \uparrow (\alpha_1 + \alpha_2)$, α and β simultaneously tend to infinity.

Remark 1. If $\alpha_3 \geq 0$ is additionally required, then $\alpha + \beta \geq 1$ must be appended in Definition 2. On the other hand, if we allow α_1 and α_2 to be negative, then β and α can be negative as well. Negative values for α_1 (resp. α_2) imply that $q(\boldsymbol{\theta})$ is expected to be far away from $p(\boldsymbol{\theta})$ [resp. $l(\boldsymbol{\theta})$]. Without loss of practicality, this paper focuses on the specifications in Assumption 1. \square

Table 1 gives illustrative examples of the (α, β) -posterior; for detailed technical conditions, derivations, and insights, see Appendix C in supplementary materials.

Table 1: Particular Examples of (α, β) -Posterior.

Name	Definition	Name	Definition
α -posterior	$p(\boldsymbol{\theta}) \cdot l^\alpha(\boldsymbol{\theta})$	α -prior	$p^\alpha(\boldsymbol{\theta})$
β -posterior	$p^\beta(\boldsymbol{\theta}) \cdot l(\boldsymbol{\theta})$	α -likelihood	$l^\alpha(\boldsymbol{\theta})$
γ -posterior	$p^\gamma(\boldsymbol{\theta}) \cdot l^\gamma(\boldsymbol{\theta})$	α -pooled posterior	$p^\alpha(\boldsymbol{\theta}) \cdot l^{1-\alpha}(\boldsymbol{\theta})$

Note: In α -pooled posterior, $\alpha \in [0, 1]$; other α , β , and γ take values on $[0, \infty)$.

2.2 Properties of Generalized Bayes' Rule

The definition of the (α, β) -posterior motivates us to study the properties of α -scaled distributions.

Definition 3 (α -Scaled Distribution). The α -scaled distribution $h^{(\alpha)}(\boldsymbol{\theta})$ induced by the distribution $h(\boldsymbol{\theta})$ is defined as

$$h^{(\alpha)}(\boldsymbol{\theta}) := \frac{h^\alpha(\boldsymbol{\theta})}{\int h^\alpha(\boldsymbol{\theta}) d\boldsymbol{\theta}}, \quad (18)$$

for $0 \leq \alpha < \infty$, if $\int h^\alpha(\boldsymbol{\theta}) d\boldsymbol{\theta}$ exists. \square

As the definition implies, $h^{(\alpha)}(\boldsymbol{\theta}) \equiv h(\boldsymbol{\theta})$ for every α if $h(\boldsymbol{\theta})$ is a uniform distribution on a finite support set Θ . Inspired by (14), we investigate the relation between the entropy of $h^{(\alpha)}(\boldsymbol{\theta})$ and that of $h(\boldsymbol{\theta})$; that is, how α controls the spread of $h^{(\alpha)}$.

Theorem 2. *Let $h(\boldsymbol{\theta})$ not be a uniform distribution. The function $\alpha \mapsto \text{Ent } h^{(\alpha)}(\boldsymbol{\theta})$ is monotonically decreasing in α on $[0, \infty)$.*

Proof. See Appendix D in supplementary materials. \square

Let $E(\alpha)$ denote the entropy difference evaluated at $\alpha \in [0, \infty)$: $E(\alpha) := \text{Ent } h^{(\alpha)}(\boldsymbol{\theta}) - \text{Ent } h(\boldsymbol{\theta})$. Theorem 2 implies that $E(\alpha)$ is monotonically decreasing in α on $[0, \infty)$. In addition, it is obvious to see that $E(0) > 0$ and $E(1) = 0$. As a result, the following corollary is immediate.

Corollary 1. *If $0 \leq \alpha < 1$, then $h^{(\alpha)}(\boldsymbol{\theta})$ has larger entropy than $h(\boldsymbol{\theta})$; if $1 < \alpha < \infty$, then $h^{(\alpha)}(\boldsymbol{\theta})$ has smaller entropy than $h(\boldsymbol{\theta})$.* \square

A concrete example for Corollary 1 is as follows; for visual illustrations, see Appendices E.1 and E.2 in supplementary materials.

Example 2. Consider an one-dimensional zero-mean Gaussian density function $h(\boldsymbol{\theta}) \propto \exp(-\frac{1}{2} \frac{\boldsymbol{\theta}^2}{\sigma^2})$ where σ^2 is the variance. The α -scaled distribution is $h^{(\alpha)}(\boldsymbol{\theta}) \propto \exp(-\frac{1}{2} \frac{\boldsymbol{\theta}^2}{\sigma^2/\alpha})$. Therefore, $h^{(\alpha)}(\boldsymbol{\theta})$ is a Gaussian density function with variance σ^2/α . When $0 < \alpha < 1$, we have $\sigma^2/\alpha > \sigma^2$ and therefore $\text{Ent } h^{(\alpha)}(\boldsymbol{\theta}) > \text{Ent } h(\boldsymbol{\theta})$; when $\alpha > 1$, we have $\sigma^2/\alpha < \sigma^2$ and therefore $\text{Ent } h^{(\alpha)}(\boldsymbol{\theta}) < \text{Ent } h(\boldsymbol{\theta})$. Note that $\text{Ent } h^{(\alpha)}(\boldsymbol{\theta}) = \frac{1}{2} \ln(2\pi\sigma^2/\alpha) + \frac{1}{2}$, while $\text{Ent } h(\boldsymbol{\theta}) = \frac{1}{2} \ln(2\pi\sigma^2) + \frac{1}{2}$. \square

Theorem 2 and Corollary 1 collectively imply the following useful insight.

Insight 1 (Uncertainty Awareness in Posterior). The α -scaling operation controls the entropy (i.e., the spread) of $h^{(\alpha)}(\boldsymbol{\theta})$. Therefore, the (α, β) -posterior $p_g(\boldsymbol{\theta}|\mathbf{y}) \propto p^\beta(\boldsymbol{\theta}) \cdot l^\alpha(\boldsymbol{\theta})$ balances the relative importance between the prior distribution $p(\boldsymbol{\theta})$ and the likelihood distribution $l(\boldsymbol{\theta})$. To be specific, if the likelihood distribution is overly opportunistic (i.e., exceedingly concentrated), we use $0 \leq \alpha < 1$ so that $\text{Ent } l^{(\alpha)}(\boldsymbol{\theta})$ can be *increased* compared to $\text{Ent } l(\boldsymbol{\theta})$; in contrast, if the likelihood distribution is overly conservative (i.e., exceedingly spread), we use $\alpha > 1$ so that $\text{Ent } l^{(\alpha)}(\boldsymbol{\theta})$ can be *reduced* compared to $\text{Ent } l(\boldsymbol{\theta})$. The same operation also applies to the prior distribution, i.e., $p^{(\beta)}(\boldsymbol{\theta})$ and $p(\boldsymbol{\theta})$. Note again, that the larger the entropy of the prior or likelihood distribution is, the more spread it is, and therefore, the less impact it has on the posterior distribution. \square

Next, we study the closeness to $h(\boldsymbol{\theta})$ from $h^{(\alpha)}(\boldsymbol{\theta})$.

Theorem 3. *The closeness to $h(\boldsymbol{\theta})$ from $h^{(\alpha)}(\boldsymbol{\theta})$, i.e., $\text{KL}[h(\boldsymbol{\theta}) \| h^{(\alpha)}(\boldsymbol{\theta})]$, is a monotonically increasing function if $1 < \alpha < \infty$ and a monotonically decreasing function if $0 \leq \alpha < 1$. In addition, it is a convex function in α on $[0, \infty)$.*

Proof. See Appendix F in supplementary materials. \square

An illustration for Theorem 3 is below; for a visualization, see Appendix E.3 in supplementary materials.

Example 3. We re-visit the setup in Example 2. We have $\text{KL}[h(\boldsymbol{\theta}) \| h^{(\alpha)}(\boldsymbol{\theta})] = -\frac{1}{2} \ln(\alpha) + \frac{\alpha}{2} - \frac{1}{2}$, for $\alpha > 0$. The derivative of $\text{KL}[h(\boldsymbol{\theta}) \| h^{(\alpha)}(\boldsymbol{\theta})]$ with respect to α is $\frac{1}{2}(1 - \frac{1}{\alpha})$, which is positive if $\alpha > 1$ and negative if $0 < \alpha < 1$; the second-order derivative is $\frac{1}{2\alpha^2} > 0$. Therefore, $\text{KL}[h(\boldsymbol{\theta}) \| h^{(\alpha)}(\boldsymbol{\theta})]$ is monotonically decreasing when $0 < \alpha < 1$ and monotonically increasing when $\alpha > 1$. In addition, $\text{KL}[h(\boldsymbol{\theta}) \| h^{(\alpha)}(\boldsymbol{\theta})]$ is convex. \square

Theorem 3 implies the following useful insight.

Insight 2 (Level of Uncertainty). The more α deviates from 1, the farther to $h(\boldsymbol{\theta})$ from $h^{(\alpha)}(\boldsymbol{\theta})$. Hence, in (α, β) -posterior, the more we trust the prior distribution $p(\boldsymbol{\theta})$ [resp. the likelihood distribution $l(\boldsymbol{\theta})$], the closer the value of β (resp. α) should be to 1. \square

Insights 1 and 2 collectively suggest the usage of the (α, β) -posterior in balancing the relative importance between the prior knowledge and the data evidence; for visual illustrations, see Appendix E.4 in supplementary materials. Next, we show another property of the (α, β) -posterior that enables its practical usefulness. Let $h_0(\boldsymbol{\theta})$ be the true distribution and $h(\boldsymbol{\theta})$ the nominal distribution serving as an estimate of $h_0(\boldsymbol{\theta})$. The theorem below states that there exists some $\alpha \geq 0$ such that the α -scaled nominal distribution $h^{(\alpha)}(\boldsymbol{\theta})$ can be closer to the true distribution $h_0(\boldsymbol{\theta})$ than the original nominal distribution $h(\boldsymbol{\theta})$.

Theorem 4. Given distributions h_0 and h on Θ , if h is not a uniform distribution and

$$\int_{\Theta} [h_0(\boldsymbol{\theta}) - h(\boldsymbol{\theta})] \ln h(\boldsymbol{\theta}) d\boldsymbol{\theta} \neq 0, \quad (19)$$

there exists $\alpha \geq 0$ such that

$$\text{KL} [h_0(\boldsymbol{\theta}) \parallel h^{(\alpha)}(\boldsymbol{\theta})] < \text{KL} [h_0(\boldsymbol{\theta}) \parallel h(\boldsymbol{\theta})]. \quad (20)$$

Proof. See Appendix G in supplementary materials. \square

Theorem 4 indicates that, if a proper α is given, $h^{(\alpha)}$ can be a better (i.e., a more accurate) surrogate of h_0 than h . However, the parameter α cannot be theoretically specified because it depends on the underlying true but unknown distribution $h_0(\boldsymbol{\theta})$; to be specific, the best value α^* of α solves

$$\alpha^* \in \underset{\alpha \geq 0}{\text{argmin}} \text{KL} [h_0(\boldsymbol{\theta}) \parallel h^{(\alpha)}(\boldsymbol{\theta})], \quad (21)$$

which however cannot be conducted in practice. The example below provides an intuitive demonstration of Theorem 4.

Example 4. Consider $h_0 := [0.2, 0.8]$, $h := [0.4, 0.6]$, and $\alpha := 2$. We have $h^{(2)} = [0.3, 0.7]$, which is closer to h_0 than h . Then, consider $h_0 := [0.4, 0.6]$, $h := [0.2, 0.8]$, and $\alpha := 0.6$. We have $h^{(0.6)} = [0.3, 0.7]$, which is closer to h_0 than h . Third, consider a continuous case where $h_0(\theta) := \mathcal{N}(\theta; 0, \sigma_0^2)$ and $h(\theta) := \mathcal{N}(\theta; 0, \sigma^2)$. For any $\alpha > 0$, we have $h^{(\alpha)}(\theta) = \mathcal{N}(\theta; 0, \sigma^2/\alpha)$. Letting $\alpha := \sigma^2/\sigma_0^2$, we have $h^{(\alpha)}(\theta) = h_0(\theta)$; NB: α can be either larger or smaller than one. \square

Theorem 4 justifies the potential that the proposed (α, β) -posterior can outperform the conventional Bayes' rule in practice: Scaled nominal prior and likelihood distributions can be closer to the true prior and likelihood distributions, respectively, than the original unscaled nominal ones. Specifically, given the true joint distribution $p_0(\boldsymbol{\theta}, \mathbf{y})$ and its surrogate $p(\boldsymbol{\theta}, \mathbf{y})$, for a measurable bounded cost function $c : \Theta \times \mathcal{Y} \rightarrow [-M, M]$ where $0 \leq M < \infty$, we have

$$\begin{aligned} & \left| \int_{\Theta} \int_{\mathcal{Y}} c(\boldsymbol{\theta}, \mathbf{y}) p_0(\boldsymbol{\theta}, \mathbf{y}) d\boldsymbol{\theta} d\mathbf{y} - \int_{\Theta} \int_{\mathcal{Y}} c(\boldsymbol{\theta}, \mathbf{y}) p(\boldsymbol{\theta}, \mathbf{y}) d\boldsymbol{\theta} d\mathbf{y} \right| \\ & \leq M \int_{\Theta} \int_{\mathcal{Y}} |p_0(\boldsymbol{\theta}, \mathbf{y}) - p(\boldsymbol{\theta}, \mathbf{y})| d\boldsymbol{\theta} d\mathbf{y} \\ & \leq 2M \sqrt{1 - \exp(-\text{KL} [p_0(\boldsymbol{\theta}, \mathbf{y}) \parallel p(\boldsymbol{\theta}, \mathbf{y})])}. \end{aligned} \quad (22)$$

The first inequality is due to the definition of the total variation distance, while the second is due to the Bretagnolle–Huber inequality. As a result, at the given observation \mathbf{y} , we have

$$\left| \int_{\Theta} c(\boldsymbol{\theta}, \mathbf{y}) p_0(\boldsymbol{\theta}|\mathbf{y}) d\boldsymbol{\theta} - \int_{\Theta} c(\boldsymbol{\theta}, \mathbf{y}) p(\boldsymbol{\theta}|\mathbf{y}) d\boldsymbol{\theta} \right| \leq 2M \sqrt{1 - \exp(-\text{KL} [p_0(\boldsymbol{\theta}|\mathbf{y}) \parallel p(\boldsymbol{\theta}|\mathbf{y})])}. \quad (23)$$

Therefore, finding a better surrogate of $p_0(\boldsymbol{\theta}|\mathbf{y})$ is vital in controlling the deviation from the optimal cost, which can be realized by employing (α, β) -scaled generalized Bayes' rule $p_g(\boldsymbol{\theta}|\mathbf{y})$ in (17). However, the optimal parameters (α, β) cannot be theoretically specified because they depend on the true posterior distribution, and therefore on the true prior and data-generating distributions, which are unknown in practice; cf. [Medina et al. \(2022, p. 26, Lemma 1\)](#), [Wu and Martin \(2023, Section 3\)](#).

When the cost function $c(\boldsymbol{\theta}, \mathbf{y})$ is specified by the outer product of the estimation error, i.e., $c(\boldsymbol{\theta}, \mathbf{y}) := [\hat{\boldsymbol{\theta}}(\mathbf{y}) - \boldsymbol{\theta}][\hat{\boldsymbol{\theta}}(\mathbf{y}) - \boldsymbol{\theta}]^\top$, where $\hat{\boldsymbol{\theta}}(\mathbf{y})$ is an estimate of $\boldsymbol{\theta}$, the expected error covariance matrix is given by

$$\int_{\Theta} \int_{\mathbf{y}} [\hat{\boldsymbol{\theta}}(\mathbf{y}) - \boldsymbol{\theta}][\hat{\boldsymbol{\theta}}(\mathbf{y}) - \boldsymbol{\theta}]^\top p_0(\boldsymbol{\theta}, \mathbf{y}) d\boldsymbol{\theta} d\mathbf{y}. \quad (24)$$

In this case, we are particularly interested in the performance upper bound of the estimator $\hat{\boldsymbol{\theta}}(\mathbf{y})$, that is, the Bayesian Cramér–Rao lower bound of (24). When the underlying true distribution $p_0(\boldsymbol{\theta}, \mathbf{y})$ is known, the optimal estimator minimizing the expected cost in (24) is the posterior mean: i.e., $\hat{\boldsymbol{\theta}}(\mathbf{y}) := \int \boldsymbol{\theta} p_0(\boldsymbol{\theta}|\mathbf{y}) d\boldsymbol{\theta}$. In real-world operation, however, $\hat{\boldsymbol{\theta}}(\mathbf{y})$ is defined through the misspecified surrogate distribution $p(\boldsymbol{\theta}, \mathbf{y})$. Consequently, as per [Tang et al. \(2023, Eq. \(5\), Thm. 1\)](#), the corresponding Bayesian Cramér–Rao lower bound of (24) depends on $p(\boldsymbol{\theta}, \mathbf{y})$, and this bound can be straightforwardly improved by [Theorem 4](#) because the definition of the pseudo-true parameter can be refined; for technical details, just compare [Tang et al. \(2023, Eq. \(5\)\)](#) with (20).

2.3 Generalized Bayes' Rule for Multiple Samples

When we have more than one sample, e.g., n i.i.d. samples $\{\mathbf{y}_1, \mathbf{y}_2, \dots, \mathbf{y}_n\}$, we can straightforwardly generalize (14) to

$$\min_{q(\boldsymbol{\theta})} \alpha_3 \text{Ent } q(\boldsymbol{\theta}) + \alpha_1 \text{KL}[q(\boldsymbol{\theta}) \| p(\boldsymbol{\theta})] + \frac{\alpha_2}{n} \sum_{i=1}^n \text{KL}[q(\boldsymbol{\theta}) \| l_{\mathbf{y}_i}(\boldsymbol{\theta})]. \quad (25)$$

The solution of (25) is given in the corollary below.

Corollary 2 (Multi-Sample Generalized Bayes' Rule). *The generalized Bayes' posterior solving (25) for n i.i.d. samples is given by*

$$p_g(\boldsymbol{\theta}|\mathbf{y}_1, \dots, \mathbf{y}_n) \propto p^{\frac{\alpha_1}{\alpha_1 + \alpha_2 - \alpha_3}}(\boldsymbol{\theta}) \cdot \left[\prod_{i=1}^n l_{\mathbf{y}_i}^{\frac{1}{n}}(\boldsymbol{\theta}) \right]^{\frac{\alpha_2}{\alpha_1 + \alpha_2 - \alpha_3}}, \quad (26)$$

if $\alpha_1 + \alpha_2 > \alpha_3$, provided that the right-hand-side term is integrable on Θ . When $\alpha_1 + \alpha_2 = \alpha_3$, $p_g(\boldsymbol{\theta}|\mathbf{y}_1, \dots, \mathbf{y}_n)$ is an arbitrary distribution supported on the set Θ^* where $\Theta^* := \text{argmax}_{\boldsymbol{\theta}} \alpha_1 \ln p(\boldsymbol{\theta}) + \alpha_2 \cdot \frac{1}{n} \sum_{i=1}^n \ln l_{\mathbf{y}_i}(\boldsymbol{\theta})$ contains all weighted maximum posterior estimates; if further $\alpha_1 = 0$, it reduces to maximum likelihood estimation. \square

The (α, β) -posterior in [Definition 2](#) under n i.i.d. samples, induced by (26), can be rewritten as

$$p_g(\boldsymbol{\theta}|\mathbf{y}_1, \dots, \mathbf{y}_n) \propto p^\beta(\boldsymbol{\theta}) \cdot \prod_{i=1}^n l_{\mathbf{y}_i}^{\frac{\alpha}{n}}(\boldsymbol{\theta}), \quad 0 \leq \alpha, \beta \leq \infty. \quad (27)$$

Table 1 can be restated accordingly; we do not repeat here.

2.4 Generalized Bayes' Rule for Multiple Priors and Samples

We can further extend (25) when multiple priors are present:

$$\min_{q(\boldsymbol{\theta})} \alpha_3 \text{Ent } q(\boldsymbol{\theta}) + \alpha_1 \left[\sum_{i=1}^m \beta_i \cdot \text{KL} [q(\boldsymbol{\theta}) \| p_i(\boldsymbol{\theta})] \right] + \alpha_2 \left[\frac{1}{n} \sum_{i=1}^n \text{KL} [q(\boldsymbol{\theta}) \| l_{\mathbf{y}_i}(\boldsymbol{\theta})] \right], \quad (28)$$

where m priors $p_1(\boldsymbol{\theta}), p_2(\boldsymbol{\theta}), \dots, p_m(\boldsymbol{\theta})$ are available with weights $\beta_1, \beta_2, \dots, \beta_m$, respectively; $\beta_i \in [0, 1]$ for every $i \in [m]$ and $\sum_{i=1}^m \beta_i = 1$.

The solution of (28) is given in the corollary below.

Corollary 3 (Multi-Prior-Multi-Sample Generalized Bayes' Rule). *The generalized Bayes' posterior solving (28) for m priors and n i.i.d. samples is given by*

$$p_g(\boldsymbol{\theta} | \mathbf{y}_1, \dots, \mathbf{y}_n) \propto \left[\prod_{i=1}^m p_i^{\beta_i}(\boldsymbol{\theta}) \right]^{\frac{\alpha_1}{\alpha_1 + \alpha_2 - \alpha_3}} \cdot \left[\prod_{i=1}^n l_{\mathbf{y}_i}^{\frac{1}{n}}(\boldsymbol{\theta}) \right]^{\frac{\alpha_2}{\alpha_1 + \alpha_2 - \alpha_3}}, \quad (29)$$

if $\alpha_1 + \alpha_2 > \alpha_3$, provided that the right-hand-side term is integrable on Θ . When $\alpha_1 + \alpha_2 = \alpha_3$, $p_g(\boldsymbol{\theta} | \mathbf{y}_1, \dots, \mathbf{y}_n)$ is an arbitrary distribution supported on the set Θ^* where $\Theta^* := \text{argmax}_{\boldsymbol{\theta}} \alpha_1 \sum_{i=1}^m \beta_i \cdot \ln p_i(\boldsymbol{\theta}) + \alpha_2 \sum_{i=1}^n \frac{1}{n} \cdot \ln l_{\mathbf{y}_i}(\boldsymbol{\theta})$ contains all weighted maximum posterior estimates. \square

The (α, β) -posterior in Definition 2 under m priors and n i.i.d. samples, induced by (29), can be rewritten as

$$p_g(\boldsymbol{\theta} | \mathbf{y}_1, \dots, \mathbf{y}_n) \propto \prod_{i=1}^m p_i^{\beta \cdot \beta_i}(\boldsymbol{\theta}) \cdot \prod_{i=1}^n l_{\mathbf{y}_i}^{\frac{\alpha}{n}}(\boldsymbol{\theta}), \quad 0 \leq \alpha, \beta \leq \infty. \quad (30)$$

Table 1 can be restated accordingly; we do not repeat here.

2.5 Examples of Application

The generalized (or uncertainty-aware) Bayes' rule (17), i.e., the (α, β) -posterior, has several potential applications in statistical machine learning and statistical signal processing. We specifically discuss classification and estimation problems. Suppose that the true joint distribution is $p_0(\mathbf{y}, \boldsymbol{\theta})$, the true prior distribution is $p_0(\boldsymbol{\theta})$, and the true likelihood distribution is $l_{0, \mathbf{y}}(\boldsymbol{\theta})$ under the measurement \mathbf{y} . Let the nominal prior distribution and the nominal likelihood distribution be $p(\boldsymbol{\theta})$ and $l_{\mathbf{y}}(\boldsymbol{\theta})$, respectively.

Bayesian Classification

Classification is a fundamental component of statistical machine learning. Let $\Theta := \{1, 2, 3, \dots, r\}$ be a categorical set where the integer r is finite. The Bayes classifier

based on the conventional Bayes' rule is $\hat{\theta}(\mathbf{y}) := \operatorname{argmax}_{\theta \in \Theta} \log p_0(\theta) + \log l_{0,\mathbf{y}}(\theta)$. In practice, however, the true distributions $p_0(\theta)$ and $l_{0,\mathbf{y}}(\theta)$ are unknown. By employing the nominal distributions $p(\theta)$ and $l_{\mathbf{y}}(\theta)$, the generalized Bayes classifier based on the (α, β) -posterior (17) can be obtained as

$$\hat{\theta}_g(\mathbf{y}) := \operatorname{argmax}_{\theta \in \Theta} \beta \log p(\theta) + \alpha \log l_{\mathbf{y}}(\theta), \quad (31)$$

which is equivalent, in the sense of the same classifier, to

$$\hat{\theta}_g(\mathbf{y}) := \operatorname{argmax}_{\theta \in \Theta} (1 - \lambda) \log p(\theta) + \lambda \log l_{\mathbf{y}}(\theta), \quad (32)$$

for $\lambda := \alpha/(\alpha + \beta)$. As we can see, for classification problems, the (α, β) -posterior with $\alpha, \beta \in [0, \infty)$ has the same effect as the $(\lambda, 1 - \lambda)$ -posterior with $\lambda \in [0, 1]$; only the ratio α/β matters. The same effect can also be achieved by the (α/β) -posterior in (4).

Bayesian Estimation

Estimation aims to infer an unknown parameter θ based on measured data \mathbf{y} . It is of particular importance in statistical signal processing. Upon collecting \mathbf{y} , the Bayes estimator in the minimum mean-squared error (MMSE) sense based on the conventional Bayes' rule is $\hat{\theta}(\mathbf{y}) := \int \theta p_0(\theta|\mathbf{y}) d\theta$, where $p_0(\theta|\mathbf{y}) \propto p_0(\theta, \mathbf{y})$ is the true Bayes' posterior distribution. In practice, however, the true distributions $p_0(\theta)$ and $l_{0,\mathbf{y}}(\theta)$ are unknown. By employing the nominal distributions $p(\theta)$ and $l_{\mathbf{y}}(\theta)$, the generalized Bayes MMSE estimator based on the (α, β) -posterior (17) can be obtained as

$$\hat{\theta}_g(\mathbf{y}) := \int \theta p_g(\theta|\mathbf{y}) d\theta. \quad (33)$$

Other Examples

In this subsection, we discuss other applications of the (α, β) -posterior. First, we give an example of application in statistical signal processing.

Example 5 (Uncertainty-Aware Particle Filter). Suppose that Θ is a finite discrete set containing r points (each point is known as a particle): i.e., $\Theta := \{\theta_1, \theta_2, \dots, \theta_r\}$. For each particle θ_i , $i \in [r]$, the likelihood evaluated at the measurement \mathbf{y} is assumed to be $p(\mathbf{y}|\theta_i)$. Further, we suppose that the prior distribution is $\mathbf{p} := [p_1, p_2, \dots, p_r]$ and the \mathbf{y} -likelihood distribution (recall Definition 1) is $\mathbf{l} := [l_1, l_2, \dots, l_r]$. Then the generalized Bayes' posterior, i.e., the (α, β) -posterior, of particles is equal to $p_g(\theta_i|\mathbf{y}) \propto p_i^\beta \cdot l_i^\alpha$, for every $i \in [r]$. The above formula leads to the uncertainty-aware particle filter for dynamic stochastic nonlinear systems. \square

Second, we give an example of application in statistical machine learning. It is shown that the uncertainty-aware Maximum *A-Posteriori* (MAP) estimation can lead to the popular ridge regression.

Example 6 (Uncertainty-Aware MAP Estimation). We consider a nonlinear regression model $y = f(\mathbf{x}; \boldsymbol{\theta}) + \epsilon$ where $y \in \mathbb{R}$ is the response, $\mathbf{x} \in \mathbb{R}^l$ is the feature vector, $\epsilon \sim \mathcal{N}(0, 1)$ is the regression error, and $\boldsymbol{\theta}$ is the parameter vector. Supposing the prior distribution of $\boldsymbol{\theta}$ is $\mathcal{N}(\mathbf{0}, \mathbf{I}_d)$, upon the collection of the data (y, \mathbf{x}) , the MAP estimator of $\boldsymbol{\theta}$ is $\min_{\boldsymbol{\theta} \in \Theta} [y - f(\mathbf{x}; \boldsymbol{\theta})]^2 + \boldsymbol{\theta}^\top \boldsymbol{\theta}$. By using the (α, β) -posterior rule, the uncertainty-aware MAP estimator of $\boldsymbol{\theta}$ can be written as $\min_{\boldsymbol{\theta} \in \Theta} \alpha [y - f(\mathbf{x}; \boldsymbol{\theta})]^2 + \beta \boldsymbol{\theta}^\top \boldsymbol{\theta}$. By letting $\lambda := \beta/\alpha$, we have the λ -ridge regression $\min_{\boldsymbol{\theta} \in \Theta} [y - f(\mathbf{x}; \boldsymbol{\theta})]^2 + \lambda \boldsymbol{\theta}^\top \boldsymbol{\theta}$. Therefore, the popular ridge regression method in statistical machine learning can be interpreted as an uncertainty-aware MAP estimation. \square

Third, we discuss an example of application that is popular in both statistical signal processing and statistical machine learning.

Example 7 (Uncertainty-Aware Bayesian Model Averaging). Suppose that we have r models indexed by $\{\theta_1, \theta_2, \dots, \theta_r\}$ to account for a signal processing or a machine learning problem. Let the prior distribution of models be $\mathbf{p} := [p_1, p_2, \dots, p_r]$ and the likelihood distribution (recall Definition 1) be $\mathbf{l} := [l_1, l_2, \dots, l_r]$. Then the generalized Bayes' posterior, i.e., the (α, β) -posterior, of models is equal to $p_g(\theta_i | \mathbf{y}) \propto p_i^\beta \cdot l_i^\alpha$, for every $i \in [r]$. The above formula induces the uncertainty-aware Bayesian model averaging method. \square

2.6 Hyper-Parameter Tuning

This subsection discusses the determination methods for the hyper-parameters (α, β) in practice. The main purpose is to find some (α, β) such that the (α, β) -posterior can outperform the conventional Bayes' posterior; cf. Theorem 4.

Let $\boldsymbol{\omega} := [\alpha, \beta]^\top$ denote the parameter vector of an (α, β) -posterior and $f(\boldsymbol{\omega})$ the loss function of using the (α, β) -posterior for a specific application, where $f : \mathbb{R}_+^2 \rightarrow \mathbb{R}$. We assume that $\boldsymbol{\omega}$ takes values on $[0, \tau]^2$ where $\tau > 1$ is a bounded positive real number (for example, $\tau = 5$). The optimal parameter tuning for $\boldsymbol{\omega}$ can be formulated as a minimization problem

$$\min_{\boldsymbol{\omega} \in [0, \tau]^2} f(\boldsymbol{\omega}). \quad (34)$$

Examples of $f(\boldsymbol{\omega})$ are given below.

Example 8 (Classification). For classification problems, the loss function is the misclassification probability, i.e.,

$$f(\boldsymbol{\omega}) := \int \int \mathbb{I}_{\{\theta \neq \hat{\theta}_{g, \boldsymbol{\omega}}(\mathbf{y})\}} \cdot p_0(\mathbf{y}, \boldsymbol{\theta}) d\mathbf{y} d\boldsymbol{\theta}, \quad (35)$$

where $\mathbb{I}_{\{\cdot\}}$ denotes the indicator function and the generalized classifier $\hat{\theta}_{g, \boldsymbol{\omega}}(\mathbf{y})$ is defined in (31). Note that $\hat{\theta}_g(\mathbf{y})$ in (31) depends on $\boldsymbol{\omega}$. If the classification method in (32) is employed, we have the cost function

$$f(\lambda) := \int \int \mathbb{I}_{\{\theta \neq \hat{\theta}_{g, \lambda}(\mathbf{y})\}} \cdot p_0(\mathbf{y}, \boldsymbol{\theta}) d\mathbf{y} d\boldsymbol{\theta}, \quad \lambda \in [0, 1]$$

since the classifier defined in (32) is parameterized by λ . \square

Example 9 (Estimation). For estimation problems, the loss function in the mean squared error (MSE) sense can be written as

$$f(\boldsymbol{\omega}) := \int \int [\boldsymbol{\theta} - \hat{\boldsymbol{\theta}}_{g,\boldsymbol{\omega}}(\mathbf{y})]^\top [\boldsymbol{\theta} - \hat{\boldsymbol{\theta}}_{g,\boldsymbol{\omega}}(\mathbf{y})] \cdot p_0(\mathbf{y}, \boldsymbol{\theta}) d\mathbf{y} d\boldsymbol{\theta}, \quad (36)$$

where the generalized estimator $\hat{\boldsymbol{\theta}}_{g,\boldsymbol{\omega}}(\mathbf{y})$ is defined in (33). Note that $\hat{\boldsymbol{\theta}}_g(\mathbf{y})$ in (33) depends on $\boldsymbol{\omega}$. \square

In practice, however, the loss function $f(\boldsymbol{\omega})$ is unknown due to the unavailability of $p_0(\mathbf{y}, \boldsymbol{\theta})$. Based on the historical data $\mathcal{D}_t := \{(\boldsymbol{\theta}_1, \mathbf{y}_1), (\boldsymbol{\theta}_2, \mathbf{y}_2), \dots, (\boldsymbol{\theta}_t, \mathbf{y}_t)\}$, we can use data-driven estimate $\hat{f}(\boldsymbol{\omega})$ as a surrogate of $f(\boldsymbol{\omega})$. For instance,

$$\hat{f}(\boldsymbol{\omega}) = \frac{1}{t} \sum_{i=1}^t \mathbb{I}_{\{\boldsymbol{\theta}_i \neq \hat{\boldsymbol{\theta}}_{g,\boldsymbol{\omega}}(\mathbf{y}_i)\}} \quad (37)$$

in Example 8 and

$$\hat{f}(\boldsymbol{\omega}) = \frac{1}{t} \sum_{i=1}^t [\boldsymbol{\theta}_i - \hat{\boldsymbol{\theta}}_{g,\boldsymbol{\omega}}(\mathbf{y}_i)]^\top [\boldsymbol{\theta}_i - \hat{\boldsymbol{\theta}}_{g,\boldsymbol{\omega}}(\mathbf{y}_i)] \quad (38)$$

in Example 9. When the training data set \mathcal{D}_t is sufficiently large, $\hat{f}(\boldsymbol{\omega})$ can be a point-wisely good estimate of $f(\boldsymbol{\omega})$.

In the following, we suggest two empirical methods for tuning $\boldsymbol{\omega}$. Since (34) is a low-dimensional optimization problem with at most two variables on a hyper-cube domain [cf. (32) and (33)], both methods can be statistically and computationally efficient; for empirical validation, see experiments in Subsection 2.7.

Grid Search

For simplicity in operation, we can generate a two-dimensional uniform grid Ω_{grid} on $[0, \tau]^2$ to obtain discrete empirical evaluations $\hat{f}(\boldsymbol{\omega})$ for $\boldsymbol{\omega} \in \Omega_{\text{grid}} \subset [0, \tau]^2$; note that $(1, 1)$ should be included in Ω_{grid} . Then, we solve $(\alpha^*, \beta^*) = \operatorname{argmin}_{\boldsymbol{\omega} \in \Omega_{\text{grid}}} \hat{f}(\boldsymbol{\omega})$ to obtain the best parameter pair (α^*, β^*) . Since $(1, 1) \in \Omega_{\text{grid}}$, we have $\hat{f}([\alpha^*, \beta^*]^\top) \leq \hat{f}([1, 1]^\top)$. Namely, the loss under the proposed (α, β) -posterior is no larger than that under the usual Bayes' posterior. This can empirically but sufficiently validate the advantage of the (α, β) -posterior over the conventional Bayes' posterior and the α -posterior.

Surrogate Optimization

The grid search method cannot pursue the global optimality on $[0, \tau]^2$. Considering the optimization problem (34) and its characteristics (i.e., f is unknown but some noisy evaluations \hat{f} are available), we can leverage the surrogate optimization frameworks,

for example, radial-basis-function surrogate optimization (Shen and Shoemaker, 2020), Gaussian-process surrogate optimization (i.e., Bayesian optimization) (Wang et al., 2023; Garnett, 2023). To put it simply, surrogate optimization uses as few as possible noisy evaluations $\hat{f}(\omega)$ to learn the true function $f(\omega)$ in an online manner, and simultaneously search for the globally optimal minimizer(s) ω^* such that $f(\omega^*) \leq f(\omega)$ for all ω on $[0, \tau]^2$.

2.7 Concrete Applications and Experiments

This subsection presents simulated and real-world experiments on classification and estimation tasks, in machine learning and signal processing, to show the superiority of the generalized (α, β) -posterior (10) over the conventional Bayes' posterior (1) and the α -posterior (4); see Figure 1 for a visual summary. In particular, the uncertainty-aware Bayes classifier, the uncertainty-aware Kalman filter, the uncertainty-aware particle filter, and the uncertainty-aware interactive-multiple-model filter are suggested and experimentally validated. For detailed experimental setups, results, discussions, and insights, see Appendix H in supplementary materials.

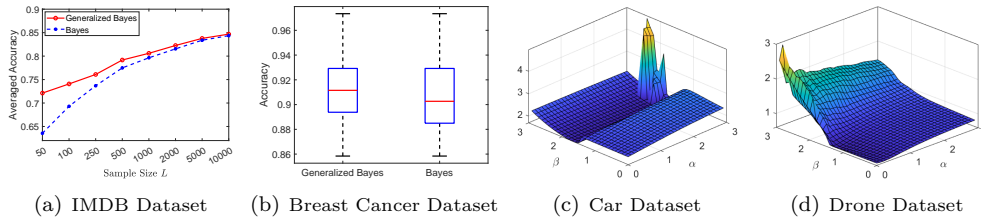


Figure 1: Experimental results on real-world data sets. (a) and (b): Classification problems in machine learning; (c) and (d): Estimation problems in signal processing. (a) Text classification on IMDB dataset. (b) Image classification on UCI Breast Cancer data set. (c) Target tracking (i.e., position and velocity estimation) results of a car; the smallest tracking error comes with $(\alpha, \beta) = (2, 1.7)$. (d) Target tracking results of a drone; the smallest tracking error comes with $(\alpha, \beta) = (0.2, 1.2)$.

3 Conclusions

To combat the potential model misspecifications in prior distributions (i.e., prior belief) and/or data distributions (i.e., data evidence), we propose to generalize the conventional Bayes' rule to the uncertainty-aware Bayes' rule. The uncertainty-aware Bayes' rule balances the relative importance of the prior distribution and the likelihood distribution by simply taking the exponentiation of the prior distribution and the likelihood distribution. We show that this exponentiation operator essentially adjusts the entropy (i.e., the concentration, the spread) of the prior distribution and the likelihood distribution. Therefore, with different exponents, the prior distribution and/or the likelihood

distribution can be upweighted (i.e., by reducing the entropy) or downweighted (i.e., by inflating the entropy) in computing the posterior. Compared to the existing maximum entropy scheme and the Rule-of-Three framework, the uncertainty-aware Bayes' rule does not introduce much additional computational burden because the exponentiation operation is computationally lightweight. In addition, compared to the existing maximum entropy scheme and α -posterior scheme, the uncertainty-aware Bayes' rule is able to combat the conservativeness (i.e., upweight the useful distributional information) of the employed prior distributions and the likelihood distributions. Simulated and real-world applications further advocate that both opportunism and conservatism are potentially useful in practice. However, the optimal parameters (α, β) cannot be theoretically specified because they depend on true prior distribution and data-generating distribution, which are unknown in practice. Therefore, the grid search and surrogate-optimization-based methods can be used to find the best values empirically.

Supplementary Material

Supplementary Materials.pdf. All appendices are placed in the supplementary materials, including 1) the technical proofs of theorems and lemmas, and 2) additional illustrative examples and visual arts for better readability.

References

- Alquier, P. and Ridgway, J. (2020). "Concentration of tempered posteriors and of their variational approximations." *The Annals of Statistics*, 48(3): 1475–1497. URL <https://doi.org/10.1214/19-AOS1855> 3, 2
- Anderson, B. D. and Moore, J. B. (1979). *Optimal Filtering*. Prentice-Hall, N.J. 13
- Arulampalam, M. S., Maskell, S., Gordon, N., and Clapp, T. (2002). "A tutorial on particle filters for online nonlinear/non-Gaussian Bayesian tracking." *IEEE Transactions on Signal Processing*, 50(2): 174–188. 14
- Bar-Shalom, Y., Challa, S., and Blom, H. A. (2005). "IMM estimator versus optimal estimator for hybrid systems." *IEEE Transactions on Aerospace and Electronic Systems*, 41(3): 986–991. 16
- Berger, J. O. (1994). "An overview of robust Bayesian analysis." *Test*, 3(1): 5–124. 2
- Blei, D. M., Kucukelbir, A., and McAuliffe, J. D. (2017). "Variational inference: A review for statisticians." *Journal of the American Statistical Association*, 112(518): 859–877. 2
- Blom, H. A. and Bar-Shalom, Y. (1988). "The interacting multiple model algorithm for systems with Markovian switching coefficients." *IEEE Transactions on Automatic Control*, 33(8): 780–783. 16
- Bordignon, V., Matta, V., and Sayed, A. H. (2021). "Adaptive social learning." *IEEE Transactions on Information Theory*, 67(9): 6053–6081. 4

- Carlin, B. P., Polson, N. G., and Stoffer, D. S. (1992). "A Monte Carlo approach to nonnormal and nonlinear state-space modeling." *Journal of the American Statistical Association*, 87(418): 493–500. 14
- Garnett, R. (2023). *Bayesian Optimization*. Cambridge University Press. 18
- Gelman, A., Carlin, J. B., Stern, H. S., and Rubin, D. B. (2013). *Bayesian Data Analysis*. Chapman and Hall/CRC, 3rd edition. 2
- Ghosal, S. and Van der Vaart, A. (2017). *Fundamentals of Nonparametric Bayesian Inference*, volume 44. Cambridge University Press. 3, 2
- Hu, P., Bordignon, V., Vlaski, S., and Sayed, A. H. (2023). "Optimal aggregation strategies for social learning over graphs." *IEEE Transactions on Information Theory*. 4
- Huber, P. J. and Ronchetti, E. M. (2009). *Robust Statistics*. John Wiley & Sons Hoboken, NJ, USA, 2nd edition. 2, 3
- Insua, D. R. and Ruggeri, F. (2000). *Robust Bayesian Analysis*. New York: Springer. 2
- Jilkov, V. P. and Li, X. R. (2004). "Online Bayesian estimation of transition probabilities for Markovian jump systems." *IEEE Transactions on Signal Processing*, 52(6): 1620–1630. 16
- Knoblauch, J., Jewson, J., and Damoulas, T. (2022). "An optimization-centric view on Bayes' rule: Reviewing and generalizing variational inference." *Journal of Machine Learning Research*, 23(132): 1–109. 2, 3, 4, 7
- Koliander, G., El-Laham, Y., Djurić, P. M., and Hlawatsch, F. (2022). "Fusion of probability density functions." *Proceedings of the IEEE*, 110(4): 404–453. 5, 7, 4
- Li, X. R. and Jilkov, V. P. (2003). "Survey of maneuvering target tracking. Part I. Dynamic models." *IEEE Transactions on Aerospace and Electronic Systems*, 39(4): 1333–1364. 16
- Maas, A. L., Daly, R. E., Pham, P. T., Huang, D., Ng, A. Y., and Potts, C. (2011). "Learning Word Vectors for Sentiment Analysis." In *Proceedings of the 49th Annual Meeting of the Association for Computational Linguistics: Human Language Technologies*, 142–150. Portland, Oregon, USA: Association for Computational Linguistics.
URL <http://www.aclweb.org/anthology/P11-1015> 10
- Medina, M. A., Olea, J. L. M., Rush, C., and Velez, A. (2022). "On the robustness to misspecification of α -posteriors and their variational approximations." *The Journal of Machine Learning Research*, 23(1): 6579–6629. 2, 3, 4, 7, 13
- Miller, J. W. and Dunson, D. B. (2019). "Robust Bayesian inference via coarsening." *Journal of the American Statistical Association*. 7
- Nguyen, V. A., Shafieezadeh Abadeh, S., Yue, M.-C., Kuhn, D., and Wiesemann, W. (2019). "Optimistic distributionally robust optimization for nonparametric likelihood approximation." *Advances in Neural Information Processing Systems*, 32. 3

- Petersen, I. R. and Savkin, A. V. (1999). *Robust Kalman Filtering for Signals and Systems with Large Uncertainties*. Springer Science & Business Media. 2
- Rufo, M. J., Martín, J., and Pérez, C. J. (2012). “Log-Linear Pool to Combine Prior Distributions: A Suggestion for a Calibration-Based Approach.” *Bayesian Analysis*, 7(2): 411 – 438.
URL <https://doi.org/10.1214/12-BA714> 4
- Ruggeri, F., Insua, D. R., and Martín, J. (2005). “Robust Bayesian Analysis.” *Handbook of Statistics*, 25: 623–667. 2
- Scikit-learn (2024). “Naive Bayes (scikit-learn documentation).” https://scikit-learn.org/stable/modules/naive_bayes.html. 11, 12
- Shen, Y. and Shoemaker, C. A. (2020). “Global optimization for noisy expensive black-box multi-modal functions via radial basis function surrogate.” In *2020 Winter Simulation Conference (WSC)*, 3020–3031. IEEE. 18
- Shmaliy, Y. S., Lehmann, F., Zhao, S., and Ahn, C. K. (2018). “Comparing Robustness of the Kalman, H_∞ , and UFIR Filters.” *IEEE Transactions on Signal Processing*, 66(13): 3447–3458. 2
- Tang, S., LaMountain, G., Imbiriba, T., and Closas, P. (2023). “On parametric misspecified Bayesian Cramér-Rao bound: An application to linear/Gaussian systems.” In *ICASSP 2023-2023 IEEE International Conference on Acoustics, Speech and Signal Processing (ICASSP)*, 1–5. IEEE. 13
- van de Schoot, R., Depaoli, S., King, R., Kramer, B., Märtens, K., Tadesse, M. G., Vannucci, M., Gelman, A., Veen, D., Willemsen, J., et al. (2021). “Bayesian statistics and modelling.” *Nature Reviews Methods Primers*, 1(1): 1. 2
- Wang, S. (2022a). “Distributionally Robust State Estimation.” Ph.D. thesis, National University of Singapore. 2, 14
- (2022b). “Distributionally Robust State Estimation for Nonlinear Systems.” *IEEE Transactions on Signal Processing*, 70: 4408–4423. 3, 7, 15
- (2023). “Distributionally Robust State Estimation for Jump Linear Systems.” *IEEE Transactions on Signal Processing*, 3835–3851. 16, 17, 18, 19
- Wang, S., Wu, Z., and Lim, A. (2021). “Robust state estimation for linear systems under distributional uncertainty.” *IEEE Transactions on Signal Processing*, 69: 5963–5978. 14
- Wang, S. and Ye, Z.-S. (2021). “Distributionally robust state estimation for linear systems subject to uncertainty and outlier.” *IEEE Transactions on Signal Processing*, 70: 452–467. 14
- Wang, X., Jin, Y., Schmitt, S., and Olhofer, M. (2023). “Recent advances in Bayesian optimization.” *ACM Computing Surveys*, 55(13s): 1–36. 18
- Wolberg, W., Mangasarian, O., Street, N., and Street, W. (1995). “Breast Cancer Wis-

- consin (Diagnostic).” UCI Machine Learning Repository. DOI: [10.24432/C5DW2B](https://doi.org/10.24432/C5DW2B). [12](#)
- Wu, P.-S. and Martin, R. (2023). “A comparison of learning rate selection methods in generalized Bayesian inference.” *Bayesian Analysis*, 18(1): 105–132. [4](#), [7](#), [13](#)
- Zhao, S. and Liu, F. (2016). “Recursive estimation for Markov jump linear systems with unknown transition probabilities: A compensation approach.” *Journal of the Franklin Institute*, 353(7): 1494–1517. [16](#)
- Zoubir, A. M., Koivunen, V., Ollila, E., and Muma, M. (2018). *Robust Statistics for Signal Processing*. Cambridge University Press. [2](#)

Supplementary Materials

Uncertainty-Aware Bayes' Rule and Its Applications

By Shixiong Wang

Appendix A: Proof of Lemma 1

Proof. According to the optimization-centric interpretation of the Bayesian posterior distribution $p(\boldsymbol{\theta}|\mathbf{y})$ in (1), $p(\boldsymbol{\theta}|\mathbf{y})$ solves

$$\min_{q(\boldsymbol{\theta})} \text{KL}[q(\boldsymbol{\theta}) \| p(\boldsymbol{\theta})] + \mathbb{E}_{\boldsymbol{\theta} \sim q(\boldsymbol{\theta})}[-\ln p(\mathbf{y}|\boldsymbol{\theta})].$$

Let $C_{\mathbf{y}} := \int p(\mathbf{y}|\boldsymbol{\theta})d\boldsymbol{\theta}$. The above optimization problem is equivalent, in the sense of the same minimizer, to

$$\begin{aligned} & \min_{q(\boldsymbol{\theta})} \text{KL}[q(\boldsymbol{\theta}) \| p(\boldsymbol{\theta})] + \mathbb{E}_{\boldsymbol{\theta} \sim q(\boldsymbol{\theta})} \left[-\ln \frac{p(\mathbf{y}|\boldsymbol{\theta})}{C_{\mathbf{y}}} \right], \\ &= \min_{q(\boldsymbol{\theta})} \text{KL}[q(\boldsymbol{\theta}) \| p(\boldsymbol{\theta})] + \mathbb{E}_{\boldsymbol{\theta} \sim q(\boldsymbol{\theta})}[-\ln l(\boldsymbol{\theta})], \\ &= \min_{q(\boldsymbol{\theta})} \text{KL}[q(\boldsymbol{\theta}) \| p(\boldsymbol{\theta})] + \text{KL}[q(\boldsymbol{\theta}) \| l(\boldsymbol{\theta})] + \text{Ent } q(\boldsymbol{\theta}). \end{aligned}$$

This completes the proof. \square

Appendix B: Proof of Theorem 1

Proof. We have

$$\begin{aligned} & \min_{q(\boldsymbol{\theta})} \alpha_1 \text{KL}[q(\boldsymbol{\theta}) \| p(\boldsymbol{\theta})] + \alpha_2 \text{KL}[q(\boldsymbol{\theta}) \| l(\boldsymbol{\theta})] + \alpha_3 \text{Ent } q(\boldsymbol{\theta}) \\ &= \min_{q(\boldsymbol{\theta})} \int q(\boldsymbol{\theta}) \ln \frac{q^{\alpha_1 + \alpha_2}(\boldsymbol{\theta})}{p^{\alpha_1}(\boldsymbol{\theta})l^{\alpha_2}(\boldsymbol{\theta})q^{\alpha_3}(\boldsymbol{\theta})} d\boldsymbol{\theta} \\ &= \min_{q(\boldsymbol{\theta})} \int q(\boldsymbol{\theta}) \ln \frac{q^{\alpha_1 + \alpha_2 - \alpha_3}(\boldsymbol{\theta})}{p^{\alpha_1}(\boldsymbol{\theta})l^{\alpha_2}(\boldsymbol{\theta})} d\boldsymbol{\theta}. \end{aligned}$$

When $\alpha_3 = \alpha_1 + \alpha_2$, any distribution supported on Θ^* solves the above optimization problem, where Θ^* contains all maximizers of $\ln[p^{\alpha_1}(\boldsymbol{\theta})l^{\alpha_2}(\boldsymbol{\theta})]$.

When $\alpha_3 < \alpha_1 + \alpha_2$, the above optimization problem is equivalent to

$$(\alpha_1 + \alpha_2 - \alpha_3) \cdot \min_{q(\boldsymbol{\theta})} \int q(\boldsymbol{\theta}) \ln \frac{q(\boldsymbol{\theta})}{p^{\frac{\alpha_1}{\alpha_1 + \alpha_2 - \alpha_3}}(\boldsymbol{\theta}) \cdot l^{\frac{\alpha_2}{\alpha_1 + \alpha_2 - \alpha_3}}(\boldsymbol{\theta})} d\boldsymbol{\theta},$$

which is further equivalent, in the sense of the same minimizer, to

$$\min_{q(\boldsymbol{\theta})} \text{KL} \left[q(\boldsymbol{\theta}) \left\| \frac{p^{\frac{\alpha_1}{\alpha_1 + \alpha_2 - \alpha_3}}(\boldsymbol{\theta}) \cdot l^{\frac{\alpha_2}{\alpha_1 + \alpha_2 - \alpha_3}}(\boldsymbol{\theta})}{C} \right\| \right],$$

where C is the normalizer. This completes the proof. \square

Appendix C: Examples of Generalized Bayes' Rule

Below we give several motivational examples of the generalized Bayes' rule (15) or (17); the first two are well-established in existing literature of Bayesian statistics.

Example 10 (Conventional Bayesian Posterior). The conventional Bayes' rule (1) [resp. (12)] is a special case of the generalized Bayes' rule (16) [resp. (15) or (17)] when $\alpha_1 = \alpha_2 = \alpha_3$ or $\alpha = \beta = 1$. \square

Example 11 (α -Posterior). When $\alpha_2 = \alpha_3$ and $\alpha_1 > 0$, (15) reduces to

$$p_g(\boldsymbol{\theta}|\mathbf{y}) \propto p(\boldsymbol{\theta}) \cdot l^{\frac{\alpha_2}{\alpha_1}}(\boldsymbol{\theta}). \quad (39)$$

By letting $\alpha := \frac{\alpha_2}{\alpha_1}$, we obtain the α -posterior

$$p_g(\boldsymbol{\theta}|\mathbf{y}) \propto p(\boldsymbol{\theta}) \cdot l^\alpha(\boldsymbol{\theta}), \quad (40)$$

where $0 \leq \alpha < \infty$. When $\alpha_1 = 0$, $p_g(\boldsymbol{\theta}|\mathbf{y})$ is an arbitrary distribution supported on Θ^* where $\Theta^* := \operatorname{argmax}_{\boldsymbol{\theta}} \ln l(\boldsymbol{\theta})$ contains all maximum likelihood estimates. \square

The α -posterior in (40) is a well-established proposal in Bayesian statistics; see, e.g., Ghosal and Van der Vaart (2017, Sec. 6.8.5 and Sec. 8.6), Medina et al. (2022); Alquier and Ridgway (2020). Given $0 < \alpha < 1$ and several other technical regularity conditions (e.g., Θ^* is a singleton), α -posteriors can be shown to have posterior consistency (see Ghosal and Van der Vaart (2017, Thm. 6.54, Ex. 8.44) and Alquier and Ridgway (2020)), asymptotic normality (see Medina et al. (2022, Thm. 1)), and robustness against likelihood-model misspecifications (see Medina et al. (2022, Sec. 4)); however, these conditions might be practically restrictive; see Example 1 where $\alpha > 1$ is preferred.

Example 12 (β -Posterior). When $\alpha_1 = \alpha_3$ and $\alpha_2 > 0$, (15) reduces to

$$p_g(\boldsymbol{\theta}|\mathbf{y}) \propto p^{\frac{\alpha_1}{\alpha_2}}(\boldsymbol{\theta}) \cdot l(\boldsymbol{\theta}). \quad (41)$$

By letting $\beta := \frac{\alpha_1}{\alpha_2}$, we obtain the β -posterior¹

$$p_g(\boldsymbol{\theta}|\mathbf{y}) \propto p^\beta(\boldsymbol{\theta}) \cdot l(\boldsymbol{\theta}), \quad (42)$$

where $0 \leq \beta < \infty$. When $\alpha_2 = 0$, $p_g(\boldsymbol{\theta}|\mathbf{y})$ is an arbitrary distribution supported on Θ^* where $\Theta^* := \operatorname{argmax}_{\boldsymbol{\theta}} \ln p(\boldsymbol{\theta})$ contains all maximum prior estimates. \square

Compared with the α -posterior in Example 11 that modifies the likelihood distribution $l(\boldsymbol{\theta})$, the β -posterior modifies the prior distribution $p(\boldsymbol{\theta})$.

Example 13 (γ -Posterior). When $\alpha_1 = \alpha_2$ and $2\alpha_1 > \alpha_3$, (15) reduces to

$$p_g(\boldsymbol{\theta}|\mathbf{y}) \propto p^{\frac{\alpha_1}{2\alpha_1 - \alpha_3}}(\boldsymbol{\theta}) \cdot l^{\frac{\alpha_1}{2\alpha_1 - \alpha_3}}(\boldsymbol{\theta}), \quad (43)$$

¹To differentiate with the α -posterior, we name it using β .

By letting $\gamma := \frac{\alpha_1}{2\alpha_1 - \alpha_3}$, we obtain the γ -posterior²

$$p_g(\boldsymbol{\theta}|\mathbf{y}) \propto p^\gamma(\boldsymbol{\theta}) \cdot l^\gamma(\boldsymbol{\theta}), \quad (44)$$

where $0 \leq \gamma < \infty$. When $2\alpha_1 = \alpha_3$, $p_g(\boldsymbol{\theta}|\mathbf{y})$ is an arbitrary distribution supported on Θ^* where $\Theta^* := \operatorname{argmax}_{\boldsymbol{\theta}} \ln p(\boldsymbol{\theta}) + \ln l(\boldsymbol{\theta})$ contains all usual maximum *a-posteriori* estimates. \square

Compared with the α -posterior and the β -posterior, the γ -posterior modifies both the prior distribution and the likelihood distribution. The β - and γ -posteriors are new proposals of this paper and have not been studied in the literature.

Example 14 (α -Likelihood). When $\alpha_1 = 0$ and $\alpha_2 > \alpha_3$, (15) reduces to

$$p_g(\boldsymbol{\theta}|\mathbf{y}) \propto l^{\frac{\alpha_2}{\alpha_2 - \alpha_3}}(\boldsymbol{\theta}). \quad (45)$$

By letting $\alpha := \frac{\alpha_2}{\alpha_2 - \alpha_3}$, we obtain the α -likelihood

$$p_g(\boldsymbol{\theta}|\mathbf{y}) \propto l^\alpha(\boldsymbol{\theta}), \quad (46)$$

where $0 \leq \alpha < \infty$. When $\alpha_2 = \alpha_3$, $p_g(\boldsymbol{\theta}|\mathbf{y})$ is an arbitrary distribution supported on Θ^* where $\Theta^* := \operatorname{argmax}_{\boldsymbol{\theta}} \ln l(\boldsymbol{\theta})$ contains all maximum likelihood estimates. \square

In the generalized Bayes' posterior (46) induced by the α -likelihood $l^\alpha(\boldsymbol{\theta})$, the prior distribution $p(\boldsymbol{\theta})$ is completely ignored. To clarify further, we only trust the likelihood distribution with the confidence level α and absolutely distrust the prior distribution.

Example 15 (α -Prior). When $\alpha_2 = 0$ and $\alpha_1 > \alpha_3$, (15) reduces to

$$p_g(\boldsymbol{\theta}|\mathbf{y}) \propto p^{\frac{\alpha_1}{\alpha_1 - \alpha_3}}(\boldsymbol{\theta}). \quad (47)$$

By letting $\alpha := \frac{\alpha_1}{\alpha_1 - \alpha_3}$, we obtain the α -prior

$$p_g(\boldsymbol{\theta}|\mathbf{y}) \propto p^\alpha(\boldsymbol{\theta}), \quad (48)$$

where $0 \leq \alpha < \infty$. When $\alpha_1 = \alpha_3$, $p_g(\boldsymbol{\theta}|\mathbf{y})$ is an arbitrary distribution supported on Θ^* where $\Theta^* \in \operatorname{argmax}_{\boldsymbol{\theta}} \ln p(\boldsymbol{\theta})$ contains all maximum prior estimates. \square

In the generalized Bayes' posterior (48) induced by the α -prior $p^\alpha(\boldsymbol{\theta})$, the likelihood distribution $l(\boldsymbol{\theta})$ is completely ignored. To clarify further, we only trust the prior distribution with the confidence level α and absolutely distrust the likelihood distribution.

Example 16 (α -Pooled Posterior). When $\alpha_3 = 0$, (15) reduces to

$$p_g(\boldsymbol{\theta}|\mathbf{y}) \propto p^{\frac{\alpha_1}{\alpha_1 + \alpha_2}}(\boldsymbol{\theta}) \cdot l^{\frac{\alpha_2}{\alpha_1 + \alpha_2}}(\boldsymbol{\theta}). \quad (49)$$

By letting $\alpha := \alpha_1 / (\alpha_1 + \alpha_2)$, we obtain the α -pooled-posterior

$$p_g(\boldsymbol{\theta}|\mathbf{y}) \propto p^\alpha(\boldsymbol{\theta}) \cdot l^{1-\alpha}(\boldsymbol{\theta}), \quad (50)$$

where $0 \leq \alpha \leq 1$. \square

²To differentiate with the α - and β -posterior, we name it using γ .

An engineering application of (50) is reported in social learning (Bordignon et al., 2021, Eq. (7)), (Hu et al., 2023, Eq. (10)). The α -pooled-posterior in (50) is a α -log-linear pooling (Rufo et al., 2012; Koliander et al., 2022) of the prior distribution $p(\boldsymbol{\theta})$ and the likelihood distribution $l(\boldsymbol{\theta})$, which is an alternative of the linear pooling rule $\alpha p(\boldsymbol{\theta}) + (1 - \alpha)l(\boldsymbol{\theta})$. The log-linear pooling rule is standard in Bayesian statistics for fusing multiple priors (from multiple experts) to obtain an integrated prior (Rufo et al., 2012). However, the α -pooled-posterior in (50) claims that the likelihood distribution can also be used as a ‘‘prior’’ where the collected data \mathbf{y} serve as an expert. (But this data-driven expert does not insist on his/her opinion due to randomness of \mathbf{y} ; he/she is a flexible expert; instead, conventional non-data-driven experts are stubborn.) In addition, from (14), we can see that when $\alpha_3 = 0$, the entropy regularizer is removed. Therefore, it is natural to imagine that the α -pooled posterior in (50) has larger entropy than the conventional Bayes' posterior $p(\boldsymbol{\theta}|\mathbf{y})$.

From Examples 10-16, we can see that the (α, β) -posterior, compared to the conventional Bayes' posterior (when $\alpha = \beta = 1$), defines general fusing rules of the prior distribution $p(\boldsymbol{\theta})$ and the likelihood distribution $l(\boldsymbol{\theta})$; we refer to the law of defining the (α, β) -posterior as the *generalized Bayes' rule*.

Appendix D: Proof of Theorem 2

Proof. Let $C_\alpha := \int h^\alpha(\boldsymbol{\theta})d\boldsymbol{\theta}$. We have

$$\begin{aligned} \text{Ent } h^{(\alpha)}(\boldsymbol{\theta}) &= \int \frac{h^\alpha(\boldsymbol{\theta})}{\int h^\alpha(\boldsymbol{\theta})d\boldsymbol{\theta}} \cdot -\ln \frac{h^\alpha(\boldsymbol{\theta})}{\int h^\alpha(\boldsymbol{\theta})d\boldsymbol{\theta}} d\boldsymbol{\theta} \\ &= \frac{1}{C_\alpha} \int h^\alpha(\boldsymbol{\theta}) \cdot [-\ln h^\alpha(\boldsymbol{\theta}) + \ln C_\alpha] d\boldsymbol{\theta} \\ &= \ln C_\alpha + \frac{\alpha}{C_\alpha} \int h^\alpha(\boldsymbol{\theta}) \cdot -\ln h(\boldsymbol{\theta}) d\boldsymbol{\theta}. \end{aligned}$$

Therefore,

$$\begin{aligned} \frac{d \text{Ent } h^{(\alpha)}(\boldsymbol{\theta})}{d\alpha} &= \frac{\alpha}{C_\alpha^2} \cdot \left\{ \left[\int h^\alpha(\boldsymbol{\theta}) \ln h(\boldsymbol{\theta}) d\boldsymbol{\theta} \right]^2 - \right. \\ &\quad \left. \int h^\alpha(\boldsymbol{\theta}) d\boldsymbol{\theta} \cdot \int h^\alpha(\boldsymbol{\theta}) \ln h(\boldsymbol{\theta}) \ln h(\boldsymbol{\theta}) d\boldsymbol{\theta} \right\}. \end{aligned}$$

Since $h^\alpha(\boldsymbol{\theta}) \geq 0$ for every α and $\boldsymbol{\theta}$, according to the Cauchy–Schwarz inequality, we have

$$\begin{aligned} &\int \left[\sqrt{h^\alpha(\boldsymbol{\theta})} \right]^2 d\boldsymbol{\theta} \int \left[\sqrt{h^\alpha(\boldsymbol{\theta}) \cdot \ln h(\boldsymbol{\theta}) \cdot \ln h(\boldsymbol{\theta})} \right]^2 d\boldsymbol{\theta} \\ &\geq \left[\int \sqrt{h^\alpha(\boldsymbol{\theta}) \cdot h^\alpha(\boldsymbol{\theta}) \cdot \ln h(\boldsymbol{\theta}) \cdot \ln h(\boldsymbol{\theta})} d\boldsymbol{\theta} \right]^2 \\ &= \left[\int h^\alpha(\boldsymbol{\theta}) \cdot |\ln h(\boldsymbol{\theta})| d\boldsymbol{\theta} \right]^2 \\ &\geq \left[\int h^\alpha(\boldsymbol{\theta}) \cdot \ln h(\boldsymbol{\theta}) d\boldsymbol{\theta} \right]^2. \end{aligned}$$

As a result,

$$\frac{d \text{Ent } h^{(\alpha)}(\boldsymbol{\theta})}{d\alpha} \leq 0.$$

If $\alpha \neq 0$, the equality holds if and only if $h(\boldsymbol{\theta})$ is a uniform distribution. This completes the proof. \square

Appendix E: Illustrative Examples

E.1 Illustration of α -Scaled Distribution

We visualize the α -scaled distribution $h^{(\alpha)}(\boldsymbol{\theta})$ when $h(\boldsymbol{\theta})$ is discrete; see Fig. 2. As we can see, when $0 \leq \alpha < 1$, the probabilities become more balanced, while when $\alpha > 1$, they become more unbalanced.

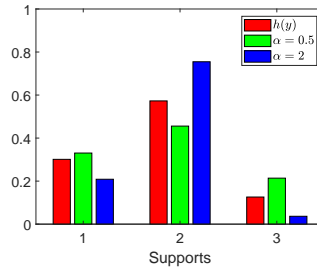


Figure 2: A 3-atom discrete distribution $h(\boldsymbol{\theta})$ and induced $h^{(\alpha)}(\boldsymbol{\theta})$ with different $\alpha \in \{0.5, 2\}$. Under $\alpha = 0.5$, $\text{Ent } h^{(\alpha)}(\boldsymbol{\theta}) > \text{Ent } h(\boldsymbol{\theta})$ (i.e., the former has more balanced masses, while the latter has more unbalanced masses). Under $\alpha = 2$, $\text{Ent } h^{(\alpha)}(\boldsymbol{\theta}) < \text{Ent } h(\boldsymbol{\theta})$.

E.2 Illustration of Entropy Difference $E(\alpha)$

A visual illustration of the entropy difference $E(\alpha)$ when $h(\boldsymbol{\theta})$ is discrete is given in Fig. 3.

E.3 Illustration of Closeness $\text{KL} [h(\boldsymbol{\theta}) \parallel h^{(\alpha)}(\boldsymbol{\theta})]$

A visual illustration of Theorem 3 when $h(\boldsymbol{\theta})$ is discrete is given in Fig. 4.

E.4 Illustration of (α, β) -Posterior

We visualize the (α, β) -posterior, compared with the conventional Bayes' posterior. We focus on a mean estimation problem where θ_0 is the true mean of the random variable y . We suppose that the prior distribution is $p(\boldsymbol{\theta}) := \mathcal{N}(\boldsymbol{\theta}; 0, 1)$. The likelihood function is

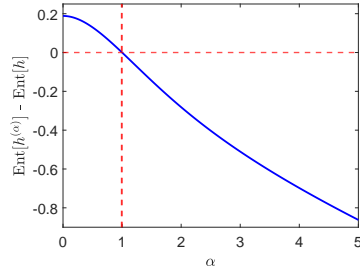


Figure 3: The entropy difference $E(\alpha) := \text{Ent} h^{(\alpha)}(\boldsymbol{\theta}) - \text{Ent} h(\boldsymbol{\theta})$ against α ; $h(\boldsymbol{\theta})$ is a randomly generated 50-atom discrete distribution.

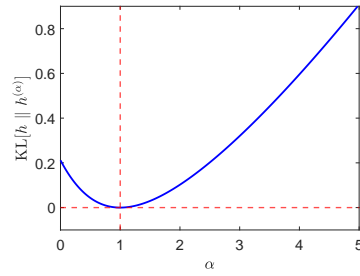


Figure 4: A visual illustration of the closeness $\text{KL} [h(\boldsymbol{\theta}) || h^{(\alpha)}(\boldsymbol{\theta})]$ to $h(\boldsymbol{\theta})$ from $h^{(\alpha)}(\boldsymbol{\theta})$; $h(\boldsymbol{\theta})$ is a randomly generated 50-atom discrete distribution.

$\theta \mapsto \mathcal{N}(y; \theta, 1)$; if we assume that the measurement is $y := 5$, the likelihood distribution is therefore $l(\theta) := \mathcal{N}(\theta; 5, 1)$. The visualizations of the (α, β) -posterior, under different value pairs of (α, β) , are given in Fig. 5.

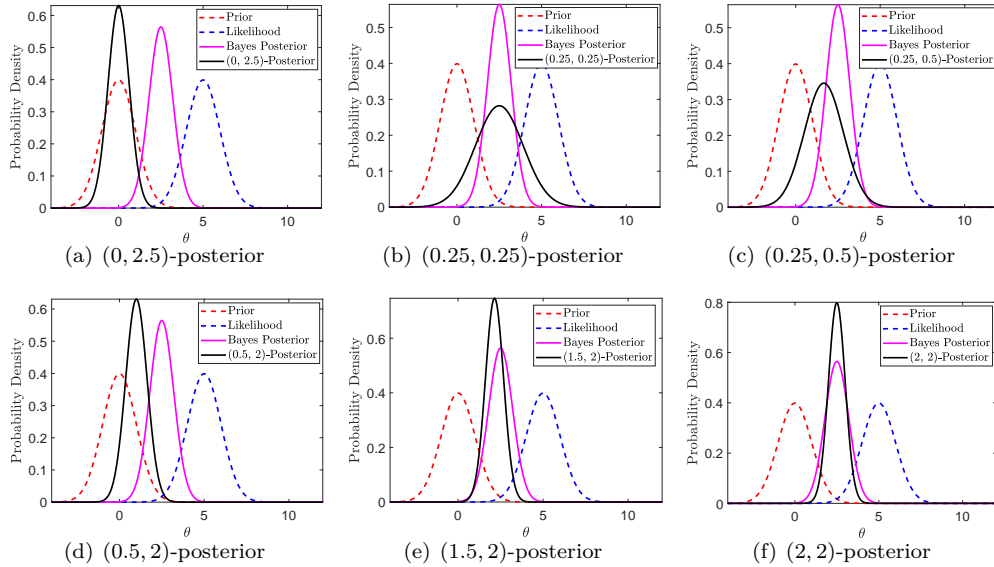


Figure 5: Illustrating examples of (α, β) -posterior. The prior distribution is $p(\theta) := \mathcal{N}(\theta; 0, 1)$. The likelihood distribution is $l_{y:=5}(\theta) := \mathcal{N}(\theta; 5, 1)$.

As motivational examples, we only interpret the first three sub-figures. In Fig. 5(a), $\alpha = 0$ means that the likelihood distribution is absolutely unreliable and the data evidence is completely ignored. Therefore, the $(0, 2.5)$ -posterior distribution tends to overlap with the prior distribution. Moreover, because $\beta = 2.5 > 1$, the specified prior distribution is thought to be overly conservative and we propose to increase its concentration. In Fig. 5(b), $\alpha = \beta = 0.25$ means that both the prior distribution and the likelihood distribution are believed to be overly opportunistic, and therefore, we propose to reduce their concentration. As a result, the $(0.25, 0.25)$ -posterior distribution has larger entropy than the conventional Bayes' posterior distribution. In Fig. 5(c), since $\alpha = 0.25 < 0.5 = \beta$, both the prior distribution and the likelihood distribution are thought to be opportunistic, but the prior distribution is thought to be less opportunistic than the likelihood distribution.

Appendix F: Proof of Theorem 3

Before proving Theorem 3, we prepare with the following lemma.

Lemma 2. *If $\alpha > 1$, then*

$$\int h^{(\alpha)}(\boldsymbol{\theta}) \ln h(\boldsymbol{\theta}) d\boldsymbol{\theta} - \int h(\boldsymbol{\theta}) \ln h(\boldsymbol{\theta}) d\boldsymbol{\theta} > 0;$$

if $\alpha < 1$, then

$$\int h^{(\alpha)}(\boldsymbol{\theta}) \ln h(\boldsymbol{\theta}) d\boldsymbol{\theta} - \int h(\boldsymbol{\theta}) \ln h(\boldsymbol{\theta}) d\boldsymbol{\theta} < 0.$$

Proof of Lemma 2. Let $C_\alpha := \int h^\alpha(\boldsymbol{\theta}) d\boldsymbol{\theta}$. Jeffrey's divergence (NB: it is symmetric) between $h(\boldsymbol{\theta})$ and $h^{(\alpha)}(\boldsymbol{\theta})$ can be given as

$$\begin{aligned} & \text{KL} [h^{(\alpha)}(\boldsymbol{\theta}) \| h(\boldsymbol{\theta})] + \text{KL} [h(\boldsymbol{\theta}) \| h^{(\alpha)}(\boldsymbol{\theta})] \\ &= \int \frac{h^{(\alpha)}(\boldsymbol{\theta})}{C_\alpha} \ln \frac{h^{(\alpha)}(\boldsymbol{\theta})}{C_\alpha \cdot h(\boldsymbol{\theta})} d\boldsymbol{\theta} + \int h(\boldsymbol{\theta}) \ln \frac{C_\alpha \cdot h(\boldsymbol{\theta})}{h^{(\alpha)}(\boldsymbol{\theta})} d\boldsymbol{\theta} \\ &= \frac{1}{C_\alpha} \left[\int h^\alpha(\boldsymbol{\theta}) \ln h^\alpha(\boldsymbol{\theta}) d\boldsymbol{\theta} - \int h^\alpha(\boldsymbol{\theta}) \ln C_\alpha d\boldsymbol{\theta} - \right. \\ & \quad \left. \int h^\alpha(\boldsymbol{\theta}) \ln h(\boldsymbol{\theta}) d\boldsymbol{\theta} \right] + \left[\int h(\boldsymbol{\theta}) \ln C_\alpha d\boldsymbol{\theta} + \right. \\ & \quad \left. \int h(\boldsymbol{\theta}) \ln h(\boldsymbol{\theta}) d\boldsymbol{\theta} - \int h(\boldsymbol{\theta}) \ln h^{(\alpha)}(\boldsymbol{\theta}) d\boldsymbol{\theta} \right] \\ &= \frac{\alpha-1}{C_\alpha} \int h^\alpha(\boldsymbol{\theta}) \ln h(\boldsymbol{\theta}) d\boldsymbol{\theta} - \ln C_\alpha + \ln C_\alpha + \\ & \quad (1-\alpha) \int h(\boldsymbol{\theta}) \ln h(\boldsymbol{\theta}) d\boldsymbol{\theta} \\ &= (\alpha-1) \left[\int h^{(\alpha)}(\boldsymbol{\theta}) \ln h(\boldsymbol{\theta}) d\boldsymbol{\theta} - \int h(\boldsymbol{\theta}) \ln h(\boldsymbol{\theta}) d\boldsymbol{\theta} \right] \\ &\geq 0. \end{aligned}$$

The equality holds if and only if $\alpha = 1$. This completes the proof. \square

Now we proceed to the proof of Theorem 3.

Proof of Theorem 3. Let $C_\alpha := \int h^\alpha(\boldsymbol{\theta}) d\boldsymbol{\theta}$. We have

$$\begin{aligned} & \text{KL} [h(\boldsymbol{\theta}) \| h^{(\alpha)}(\boldsymbol{\theta})] \\ &= \int h(\boldsymbol{\theta}) \ln \frac{h(\boldsymbol{\theta})}{h^{(\alpha)}(\boldsymbol{\theta})} d\boldsymbol{\theta} \\ &= \int h(\boldsymbol{\theta}) \ln \frac{C_\alpha \cdot h(\boldsymbol{\theta})}{h^{(\alpha)}(\boldsymbol{\theta})} d\boldsymbol{\theta} \\ &= \ln C_\alpha + (\alpha-1) \text{Ent } h(\boldsymbol{\theta}). \end{aligned}$$

Therefore,

$$\begin{aligned} & \frac{d \text{KL} [h(\boldsymbol{\theta}) \| h^{(\alpha)}(\boldsymbol{\theta})]}{d\alpha} \\ &= \int h^{(\alpha)}(\boldsymbol{\theta}) \ln h(\boldsymbol{\theta}) d\boldsymbol{\theta} + \text{Ent } h(\boldsymbol{\theta}) \\ &= \int h^{(\alpha)}(\boldsymbol{\theta}) \ln h(\boldsymbol{\theta}) d\boldsymbol{\theta} - \int h(\boldsymbol{\theta}) \ln h(\boldsymbol{\theta}) d\boldsymbol{\theta}. \end{aligned}$$

Then, by Lemma 2, the monotonicity is immediate.

In addition,

$$\begin{aligned} & \frac{d^2 \text{KL} [h(\boldsymbol{\theta}) \| h^{(\alpha)}(\boldsymbol{\theta})]}{d^2 \alpha} \\ &= \frac{1}{C_\alpha^2} \left\{ \int h^\alpha(\boldsymbol{\theta}) d\boldsymbol{\theta} \cdot \int h^\alpha(\boldsymbol{\theta}) \ln h(\boldsymbol{\theta}) \ln h(\boldsymbol{\theta}) d\boldsymbol{\theta} - \left[\int h^\alpha(\boldsymbol{\theta}) \ln h(\boldsymbol{\theta}) d\boldsymbol{\theta} \right]^2 \right\} \\ &\geq 0. \end{aligned}$$

The last inequality is due to the Cauchy–Schwarz inequality; the equality holds if and only if $h(\boldsymbol{\theta})$ is a uniform distribution; see Appendix D. This completes the proof. \square

Appendix G: Proof of Theorem 4

Proof. Let $C_\alpha := \int h^\alpha(\boldsymbol{\theta}) d\boldsymbol{\theta}$. We have

$$\begin{aligned} f(\alpha) &:= \text{KL} [h_0(\boldsymbol{\theta}) \| h(\boldsymbol{\theta})] - \text{KL} [h_0(\boldsymbol{\theta}) \| h^{(\alpha)}(\boldsymbol{\theta})] \\ &= \int h_0(\boldsymbol{\theta}) \ln \frac{h_0(\boldsymbol{\theta})}{h(\boldsymbol{\theta})} d\boldsymbol{\theta} - \int h_0(\boldsymbol{\theta}) \ln \frac{h_0(\boldsymbol{\theta}) C_\alpha}{h^\alpha(\boldsymbol{\theta})} d\boldsymbol{\theta} \\ &= \int h_0(\boldsymbol{\theta}) \ln \frac{h^\alpha(\boldsymbol{\theta})}{h(\boldsymbol{\theta}) C_\alpha} d\boldsymbol{\theta} \\ &= (\alpha - 1) \int h_0(\boldsymbol{\theta}) \ln h(\boldsymbol{\theta}) d\boldsymbol{\theta} - \ln \int h^\alpha(\boldsymbol{\theta}) d\boldsymbol{\theta}. \end{aligned}$$

Therefore,

$$\begin{aligned} \frac{df(\alpha)}{d\alpha} &= \int h_0(\boldsymbol{\theta}) \ln h(\boldsymbol{\theta}) d\boldsymbol{\theta} - \frac{\int h^\alpha(\boldsymbol{\theta}) \ln h(\boldsymbol{\theta}) d\boldsymbol{\theta}}{\int h^\alpha(\boldsymbol{\theta}) d\boldsymbol{\theta}} \\ &= \int h_0(\boldsymbol{\theta}) \ln h(\boldsymbol{\theta}) d\boldsymbol{\theta} - \int h^{(\alpha)}(\boldsymbol{\theta}) \ln h(\boldsymbol{\theta}) d\boldsymbol{\theta}. \end{aligned}$$

As a result,

$$\left. \frac{df(\alpha)}{d\alpha} \right|_{\alpha=1} = \int [h_0(\boldsymbol{\theta}) - h(\boldsymbol{\theta})] \ln h(\boldsymbol{\theta}) d\boldsymbol{\theta}.$$

In addition,

$$\begin{aligned} & \frac{d^2 f(\alpha)}{d\alpha^2} \\ &= -\frac{1}{C_\alpha^2} \left\{ \int h^\alpha(\boldsymbol{\theta}) d\boldsymbol{\theta} \cdot \int h^\alpha(\boldsymbol{\theta}) \ln h(\boldsymbol{\theta}) \ln h(\boldsymbol{\theta}) d\boldsymbol{\theta} - \right. \\ & \quad \left. \left[\int h^\alpha(\boldsymbol{\theta}) \ln h(\boldsymbol{\theta}) d\boldsymbol{\theta} \right]^2 \right\} \\ & \leq 0, \end{aligned}$$

where the last inequality is due to the Cauchy–Schwarz inequality; the equality holds if and only if $h(\boldsymbol{\theta})$ is a uniform distribution; see Appendix D.

Since $h(\boldsymbol{\theta})$ is not a uniform distribution, we have $\frac{d^2 f(\alpha)}{d\alpha^2} < 0$ for all $\alpha \geq 0$. That is, $f(\alpha)$ is strictly concave on $[0, \infty)$. In addition, we have $f(1) = 0$. Therefore, as long as $\frac{df(\alpha)}{d\alpha}|_{\alpha=1} \neq 0$, there exists $\alpha \in [0, \infty)$ such that $f(\alpha) > 0$. Note that $f(\alpha)$ is continuous in α . This completes the proof. \square

Appendix H: Concrete Applications and Experiments

The uncertainty-aware Bayes' rule (17) can give birth to several uncertainty-aware Bayesian machine learning methods and uncertainty-aware Bayesian signal processing methods. As demonstrations and without loss of generality, in this section, we focus on naive Bayes classification problems in machine learning and state estimation (i.e., state filtering) problems of dynamic stochastic state-space systems in signal processing. In particular, the uncertainty-aware Bayes classifier, the uncertainty-aware Kalman filter, the uncertainty-aware particle filter, and the uncertainty-aware interactive-multiple-model filter are suggested and experimentally validated. The main purpose is to show the existence of (α, β) such that the (α, β) -posterior can outperform the conventional Bayesian posterior; cf. Theorem 4. In addition, we aim to show that the α -posterior is not sufficient for some real-world applications, and therefore, the (α, β) -posterior is necessary. All the source data and codes are available online at GitHub: <https://github.com/Spratm-Asleaf/Bayes-Rule>. The experimental results are obtained by a Lenovo laptop with 16G RAM and 11th Gen Intel(R) Core(TM) i5-11300H CPU @ 3.10GHz.

H.1 Bayesian Classification: Text and Image Classification

We consider two real-world classification problems. One is a natural-language text classification problem, while the other is a medical image classification problem.

IMDB Dataset

We investigate the performances of the generalized Bayes classifier in (32) on the IMDB dataset containing movie reviews (Maas et al., 2011, Sec. 4.3.2). This problem is also

known as text-based sentiment analysis where we determine whether a review of a movie is positive or negative. The multinomial naive Bayes classification algorithm with Laplacian smoothing is employed; that is, the features are distributed according to multinomial distributions because movie reviews are typically represented as word vector counts, and the features are assumed to be conditionally independent given the target class; see [Scikit-learn \(2024\)](#).

For every sample size L in $\{50, 100, 250, 500, 1000, 2000, 5000, 10000\}$, we conduct 500 independent Monte–Carlo tests. In detail, in each Monte–Carlo trial, we randomly select L samples from the IMDB dataset, of which 80% are training samples and 20% are testing samples. For each Monte–Carlo test, the radial-basis-function surrogate optimization on $[0, 1]$ is employed to find the empirically optimal hyper-parameter λ in (32);³ the testing performance, which is a function of λ , serves as the loss function in (34) to be minimized. The surrogate-optimization-based search process starts with $\lambda = 0.5$ (i.e., the conventional Bayes classifier) so that the performance of the generalized Bayes classifier (32) is at least as good as that of the conventional Bayes classifier. The experimental results are shown in Fig. 6.

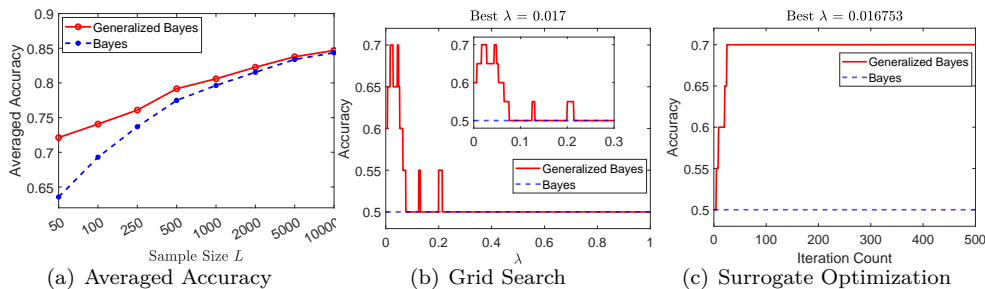


Figure 6: Experimental results on the IMDB data set. (a): The classification accuracy against sample size L , averaged over 500 Monte–Carlo episodes. (b): The grid search for λ with step size of 0.001 in a Monte–Carlo trial when $L = 100$. (c): The visual illustration of the surrogate optimization process for λ on $[0, 1]$; the found optimal value is $\lambda = 0.016753$.

As sample size L becomes larger, the nominal distributions $p(\theta)$ and $l_{\mathbf{y}}(\theta)$ get closer to the true distributions $p_0(\theta)$ and $l_{0,\mathbf{y}}(\theta)$, respectively. Therefore, the conventional Bayes classifier tends to obtain the best classification accuracy as L increases; cf. Fig. 6(a). In Figs. 6(b) and 6(c), the parameter tuning process is visualized for a Monte–Carlo trial when $L = 100$. Since the found optimal $\lambda = 0.016753$, any hyper-parameter pair of (α, β) in (31) such that $\alpha/(\alpha + \beta) = 0.016753$ is optimal. Both two tuning methods find the best accuracy of 0.7. The average running times of the two tuning methods, against sample size L , are shown in Fig. 7. Note that the larger the testing sample size, the more running time is needed to calculate the empirical performance (37).

³See MATLAB’s `surrogateopt` function: <https://mathworks.com/help/gads/surrogateopt.html>.

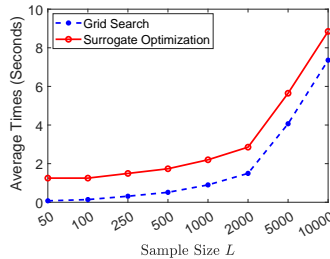


Figure 7: Average running times of the two tuning methods against sample size L . The time difference of the two tuning methods remains about 1.5 seconds for every L . The running time of grid search depends on the step size (NB: the smaller the step size, the larger the maximum accuracy, but the more the running times), while that of surrogate optimization depends on the maximum allowed iteration count (NB: the larger the iteration count, the larger the maximum accuracy, but the more the running times).

UCI Breast Cancer Dataset

We examine the performance of the generalized Bayes classifier in (32) on the UCI Breast Cancer dataset (Wolberg et al., 1995). This is an image-classification-based medical diagnosis problem. The Gaussian naive Bayes classifier is employed; that is, the features are distributed according to Gaussian distributions, and the features are assumed to be conditionally independent given the target class; see Scikit-learn (2024).

Since there are only 569 instances in this data set, we use all of them in the experiment. We conduct 500 independent Monte–Carlo tests. In each Monte–Carlo trial, 80% of the 569 instances are randomly drawn to serve as training samples, while the remaining 20% are testing samples. The radial-basis-function surrogate optimization on $[0, 1]$ is employed to find the empirically optimal hyper-parameter λ in (32); the testing performance, which is a function of λ , serves as the loss function in (34) to be minimized. The surrogate-optimization-based search process starts with $\lambda = 0.5$ (i.e., the conventional Bayes classifier) so that the performance of the generalized Bayes classifier (32) is at least as good as that of the conventional Bayes classifier. The experimental results are shown in Fig. 8(a). In a Monte–Carlo trial, both parameter tuning methods find the best accuracy of 0.9027; see Figs. 8(b) and 8(c).

Running Times: The average running time for the grid search method is 0.2 seconds and for the surrogate optimization method is 1.5 seconds.

H.2 Bayesian Estimation: State Estimation

From the perspective of applied statistics, state estimation problems can be interpreted as sequential Bayesian inference. Briefly speaking, state estimation aims to estimate the unknown (i.e., unobservable) state vector \mathbf{x}_k at the discrete time step k using the known (i.e., observable) measurement set $\mathcal{Y}_k := (\mathbf{y}_1, \mathbf{y}_2, \dots, \mathbf{y}_k)$ and the probabilistic model $p_{\mathbf{x}_k, \mathcal{Y}_k}(\mathbf{x}_k, \mathbf{Y}_k)$; the probabilistic model $p_{\mathbf{x}_k, \mathcal{Y}_k}(\mathbf{x}_k, \mathbf{Y}_k)$ is induced by the stochastic state-

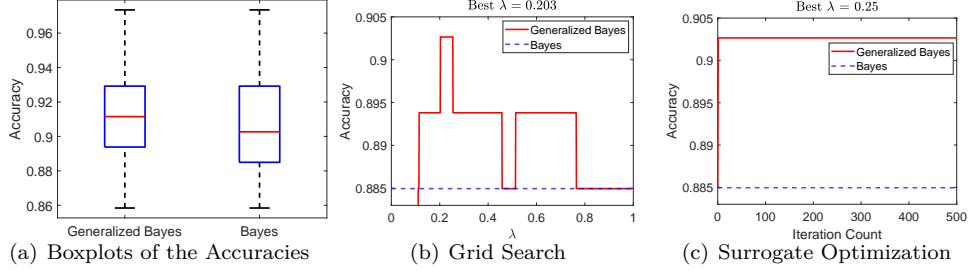


Figure 8: Experimental results on the UCI Breast Cancer data set. (a): The boxplots for the classification accuracies of 500 Monte–Carlo episodes. (b): The grid search for λ with step size of 0.001 in a Monte–Carlo trial. (c): The visual illustration of the surrogate optimization process for λ on $[0, 1]$; the found optimal value is $\lambda = 0.25$.

space models. The aim of state estimation is to obtain the posterior state distribution $p_{\mathbf{x}_k|\mathcal{Y}_k}(\mathbf{x}_k|\mathcal{Y}_k)$ or the posterior mean $\mathbb{E}(\mathbf{x}_k|\mathcal{Y}_k)$.

Uncertainty-Aware Kalman Filter

We consider the state estimation problem of linear Gaussian state-space models (Anderson and Moore, 1979, Chap. 3)

$$\begin{cases} \mathbf{x}_k &= \mathbf{F}_{k-1}\mathbf{x}_{k-1} + \mathbf{G}_{k-1}\mathbf{w}_{k-1}, \\ \mathbf{y}_k &= \mathbf{H}_k\mathbf{x}_k + \mathbf{v}_k, \end{cases} \quad (51)$$

where, for every time k , the system matrices \mathbf{F}_k , \mathbf{G}_k , and \mathbf{H}_k are assumed to be known. The process noise vector and the measurement noise vector are denoted by $\mathbf{w}_k \sim \mathcal{N}(\mathbf{0}, \mathbf{Q}_k)$ and $\mathbf{v}_k \sim \mathcal{N}(\mathbf{0}, \mathbf{R}_k)$, respectively, and \mathbf{Q}_k and \mathbf{R}_k are assumed to be known, for every k . For this linear Gaussian system, under several uncorrelatedness assumptions among \mathbf{x}_0 , $\{\mathbf{w}_k\}_{\forall k}$, and $\{\mathbf{v}_k\}_{\forall k}$ (see Anderson and Moore (1979, p. 38)), the Kalman filter is the optimal state estimator in the sense of minimum mean-squared error.

Suppose that at time $k - 1$, the posterior state distribution is

$$\hat{\mathbf{x}}_{k-1|k-1} \sim \mathcal{N}(\hat{\mathbf{x}}_{k-1|k-1}, \mathbf{P}_{k-1|k-1}).$$

At time k , the prior state distribution is

$$\hat{\mathbf{x}}_{k|k-1} \sim \mathcal{N}(\hat{\mathbf{x}}_{k|k-1}, \mathbf{P}_{k|k-1})$$

where $\mathbf{P}_{k|k-1} := \mathbf{F}_{k-1}\mathbf{P}_{k-1|k-1}\mathbf{F}_{k-1}^\top + \mathbf{G}_{k-1}\mathbf{Q}_{k-1}\mathbf{G}_{k-1}^\top$ and $\hat{\mathbf{x}}_{k|k-1} := \mathbf{F}_{k-1}\hat{\mathbf{x}}_{k-1|k-1}$; the measurement distribution conditioned on state \mathbf{x}_k is

$$\mathbf{y}_k|\mathbf{x}_k \sim \mathcal{N}(\mathbf{H}_k\mathbf{x}_k, \mathbf{R}_k).$$

Therefore, by applying the (α, β) -posterior rule (17), the prior state distribution should be modified to

$$\hat{\mathbf{x}}_{k|k-1} \sim \mathcal{N}(\hat{\mathbf{x}}_{k|k-1}, \mathbf{P}_{k|k-1}/\beta)$$

and the conditional measurement distribution should be modified to

$$\mathbf{y}_k | \mathbf{x}_k \sim \mathcal{N}(\mathbf{H}_k \mathbf{x}_k, \mathbf{R}_k/\alpha).$$

Note that for a Gaussian distribution $\mathcal{N}(\boldsymbol{\mu}, \boldsymbol{\Sigma})$, the α -scaled version is equal to $\mathcal{N}(\boldsymbol{\mu}, \boldsymbol{\Sigma}/\alpha)$. As a result, the (α, β) -uncertainty-aware Kalman filter can be accordingly obtained by just applying the following two assignment operations in each Kalman iteration: $\mathbf{P}_{k|k-1} \leftarrow \mathbf{P}_{k|k-1}/\beta$ and $\mathbf{R}_k \leftarrow \mathbf{R}_k/\alpha$, for $\alpha, \beta > 0$. The former operation admits that the state-transition equation is uncertain (thus to be compensated by β), while the latter admits that the state-measurement equation is uncertain (thus to be compensated by α).

This modification is reminiscent of the distributionally robust state estimation (DRSE) method proposed in Wang et al. (2021); see also Wang (2022a, p. 22, p. 53) for intuitive interpretations. Hence, when $0 < \alpha, \beta \leq 1$, the (α, β) -uncertainty-aware Kalman filter is equivalent to distributionally robust state estimation methods in Wang et al. (2021); Wang and Ye (2021), provided that there are no outliers in measurements. Since $0 < \alpha, \beta \leq 1$, $\mathbf{P}_{k|k-1}$ and \mathbf{R}_k are assumed to be overly opportunistic, and therefore, they need to be inflated. When $\alpha, \beta \geq 1$, the values of $\mathbf{P}_{k|k-1}$ and \mathbf{R}_k are reduced, which implies that $\mathbf{P}_{k|k-1}$ and \mathbf{R}_k are assumed to be overly conservative. However, from the technical derivations of the DRSE method, the value reduction of $\mathbf{P}_{k|k-1}$ and \mathbf{R}_k cannot be achieved in the DRSE method. In this sense, therefore, the (α, β) -uncertainty-aware Kalman filter presented in this paper generalizes the DRSE method in Wang et al. (2021); Wang and Ye (2021) when there are no measurement outliers: the former can handle not only opportunistic cases (by inflating covariances) but also conservative cases (by reducing covariances), while the latter can only address opportunistic cases. (NB: To combat opportunism is to introduce robustness/conservatism; i.e., robust methods innately cannot fight against conservatism.)

The experiments of the DRSE method in Wang (2022a, Chap. 2) can sufficiently support the practical values of the (α, β) -uncertainty-aware Kalman filter; just notice the mathematical equivalence to the DRSE method (when $0 < \alpha, \beta \leq 1$). We do not repeat these experiments here.

Uncertainty-Aware Particle Filter

The particle filter is standard to handle the state estimation problem of nonlinear systems (Arulampalam et al., 2002). By employing the (α, β) -posterior in (17), the (α, β) -uncertainty-aware particle filter can be straightforwardly obtained; see Example 5.

As an illustration, we specifically consider the state estimation problem of a 1-dimensional nonlinear system model (Carlin et al., 1992; Arulampalam et al., 2002;

Wang, 2022b)

$$\begin{cases} x_k = \frac{x_{k-1}}{2} + \frac{25x_{k-1}}{1+x_{k-1}^2} + 8 \cos(1.2k) + w_{k-1}, \\ y_k = \frac{x_k^2}{20} + 0.5 \sin(x_k) + v_k, \end{cases} \quad (52)$$

where for every k , $w_k \sim \mathcal{N}(0, 10)$ and $v_k \sim \mathcal{N}(0, 1)$; for every k_1 and k_2 , w_{k_1} and w_{k_2} are uncorrelated, so are v_{k_1} and v_{k_2} ; for every k , w_k and v_k are uncorrelated. As in Wang (2022b), we assume that the *nominal* measurement equation is

$$y_k = \frac{x_k^2}{20} + v_k,$$

which is slightly different from the true one in (52). Therefore, in this case, there is a modeling uncertainty in the measurement equation, i.e., in likelihood distributions at every k . As a result, to combat this model uncertainty and improve the filtering accuracy, we should use $\beta = 1$ and $\alpha < 1$.

For the purpose of experimental demonstration, we use 50, 100, and 200 particles, respectively, to report the performance of the $(\alpha, 1)$ -uncertainty-aware particle filter. The systematic resampling method is adopted to address particle degeneracy, and the effective sample size is set to half the number of particles. Given the number of particles, the experiment is independently conducted with 500 episodes and each episode contains 100 time steps. The performance measure, in every episode, is the rooted time-averaged mean-squared error (RTAMSE) along 100 time steps, i.e., $\sqrt{\frac{1}{100} \sum_{k=1}^{100} (x_k - \hat{x}_k)^2}$, where \hat{x}_k denotes the estimate of the true value x_k ; the overall performance measure for a given number of particles is the averaged RTAMSEs of the 500 episodes. The filtering result of the $(\alpha, 1)$ -uncertainty-aware particle filter is shown in Fig. 9, plotted against the value of α .

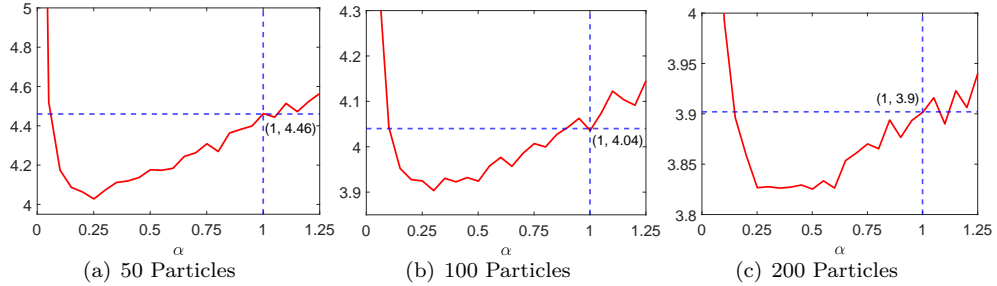


Figure 9: Averaged-RTAMSE performance of the $(\alpha, 1)$ -uncertainty-aware particle filter, against the value of α . The larger the number of particles, the smaller the averaged RTAMSE. For a given number of particles, the $(\alpha, 1)$ -uncertainty-aware particle filter with $\alpha \approx 0.25$ works best.

As we can see from Fig. 9, when $\alpha < 1$ but α is not close to zero, the $(\alpha, 1)$ -uncertainty-aware particle filter can outperform the conventional particle filter: This is

because when there exists model uncertainty in the measurement equation, the likelihood distribution of particles at each time step tends to be unreliable, and therefore, we need to reduce the concentration (i.e., reduce the trust level and improve the entropy) of the likelihood distribution to cope with the uncertainty. In addition, the results suggest that the superiority of the $(\alpha, 1)$ -uncertainty-aware particle filter tends to be more significant as the number of particles decreases: This implies that the $(\alpha, 1)$ -uncertainty-aware particle filter has the innate ability to fight against the particle degeneracy issue. When α is overly small (i.e., close to zero), the $(\alpha, 1)$ -uncertainty-aware particle filter almost ignores information from the measurements, and therefore, the filter diverges: This indicates that uncertain information is at least better than no information.

Uncertainty-Aware Interactive Multiple Model Filter

The interactive multiple model (IMM) filter is standard to handle the state estimation problem of jump linear systems (Blom and Bar-Shalom, 1988; Bar-Shalom et al., 2005). By employing the (α, β) -posterior in (17), the (α, β) -uncertainty-aware IMM filter can be straightforwardly obtained. One may just imagine the models' prior weights as a prior distribution and the models' likelihoods (evaluated at a given measurement) as a likelihood distribution; the aim is to infer the models' posterior distribution and then compute the posterior state estimate; see Example 7.

As an illustration, we consider two real-world one-dimensional multi-model target tracking problems; as claimed in Li and Jilkov (2003), focusing on only one coordinate does not lose the generality because the motions of a dynamic target in different coordinates can be independently tracked. Mathematically, it is a state estimation problem of a jump linear system model (Jilkov and Li, 2004; Zhao and Liu, 2016; Wang, 2023)

$$\begin{cases} \mathbf{x}_k = \begin{bmatrix} 1 & T \\ 0 & 1 \end{bmatrix} \mathbf{x}_{k-1} + \begin{bmatrix} T^2/2 \\ T \end{bmatrix} [a_{j_k, k-1} + w_{k-1}] \\ y_k = p_k + v_k, \end{cases}$$

where the state vector \mathbf{x}_k is defined as $\mathbf{x}_k := [p_k, s_k]^\top$; $p_k \in \mathbb{R}$ denotes the position, $s_k \in \mathbb{R}$ the speed, and $a_{j_k, k} \in \mathbb{R}$ the maneuvering acceleration of a moving target at time k ; the positive-integer-valued discrete random variable j_k denotes the system's operating mode at time k ; $T > 0$ is the sampling time between two discrete time indices; $w_k \in \mathbb{R}$ is the acceleration modeling noise and $v_k \in \mathbb{R}$ the sensor's observation noise at time k . At time k , the maneuvering acceleration may randomly take any one of the following values

$$a_{j_k, k} = \begin{cases} 0, & j_k = 1, \\ 10, & j_k = 2, \\ -10, & j_k = 3, \end{cases} \quad (53)$$

i.e., the random variable j_k randomly jumps; the diagonal elements of the transition probability matrix are set to 0.8s and the non-diagonal ones are set to 0.1s. Therefore, in state estimation for this jump linear system, at every time k , we need to jointly estimate the unknown state \mathbf{x}_k and the system's unknown operating mode j_k based on the past measurements $\{y_1, y_2, \dots, y_k\}$.

We reuse the real-world data and experimental setups from Wang (2023): In short, data from usual GPS are to be processed to obtain higher-accuracy target positions and velocities in real time, while data from RTK serve as ground truth. The RTAMSE, for the total K time steps, is computed as $\sqrt{\frac{1}{K} \sum_{k=1}^K (p_k - \hat{p}_k)^2 + (s_k - \hat{s}_k)^2}$, where p_k (resp. s_k) denotes the true value of position (resp. velocity) at the time k , and \hat{p}_k (resp. \hat{s}_k) denotes its estimate. Note that (p_k, s_k) for every k is provided by RTK. (Some authors prefer to independently report the RTAMSEs of position estimates $\{\hat{p}_k\}_{\forall k \in [K]}$ and velocity estimates $\{\hat{s}_k\}_{\forall k \in [K]}$, respectively, because the two dimensions have different numerical scales. However, the author’s experiments suggest that it introduces no essential influence on the main claims of this paper. One may use the shared source codes to verify this point.)

Track A Slowly-Maneuvering Car: We first track a slowly-maneuvering car that travels on a road in Beijing, China. The car and its trajectory are shown in Fig. 10.



Figure 10: Car and its trajectory (data credit: UniStrong Co., Ltd. and Wang (2023)).

The east axis (in the east-north-up coordinate) is investigated (Wang, 2023). The RTAMSE performance against the values of (α, β) is shown in Fig. 11.

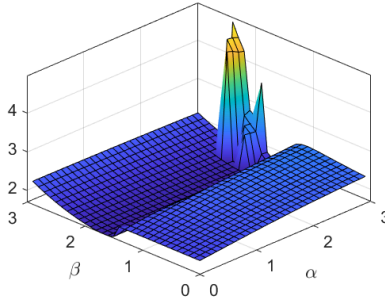


Figure 11: Averaged-RTAMSE performance of the (α, β) -uncertainty-aware IMM filter, against the values of (α, β) . The (α, β) -uncertainty-aware IMM filter with $(\alpha, \beta) = (2, 1.7)$ works best.

The results suggest that the (α, β) -uncertainty-aware IMM (IMM-UA) filter with

$(\alpha, \beta) = (2, 1.7)$ works best, under which the tracking results (RTAMSE) are shown in Table 2.

Table 2: Tracking Results of The Car: $(\alpha, \beta) = (2, 1.7)$

Filter	RTAMSE	Avg Time	Filter	RTAMSE	Avg Time
IMM	2.30	1.05e-05	IMM-UA	1.69	1.07e-05

Avg Time: Average Execution Time at each time step (unit: seconds).

From Table 2, we can see that the value pair of $(\alpha, \beta) = (2, 1.7)$ significantly reduces the tracking errors for the car. This value pair concentrates both the prior distribution (i.e., prior model weights) and the likelihood distribution (i.e., model likelihoods), which means that one of the three models in (53) dominates the rest two models most of the time. This implication coincides with our intuition from Fig. 10(b) that most of the time k , the model with $a_{1,k} = 0$ (i.e., constant velocity and straight-line trajectory) dominates the motion of the car.

Track A Highly-Maneuvering Drone: We next track a highly-maneuvering drone that flies following round trajectories in the air over an open playground, with a flying speed of about 6m/s during data collection. The drone and parts of its trajectory are shown in Fig. 12.

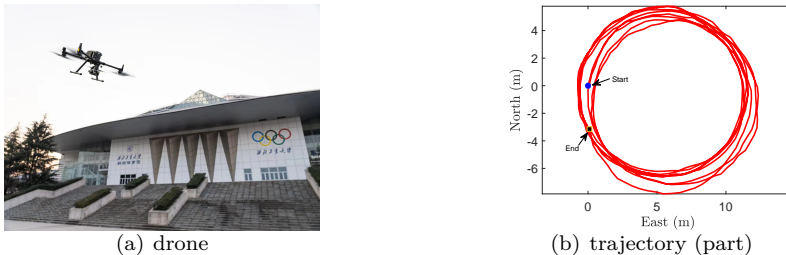


Figure 12: Drone and its flying trajectory, starting from 10s and ending at 60s (data credit: Northwestern Polytechnical University and Wang (2023)).

The east axis (in the east-north-up coordinate) is investigated (Wang, 2023). The RTAMSE performance against the values of (α, β) is shown in Fig. 13.

The results suggest that the (α, β) -uncertainty-aware IMM filter with $(\alpha, \beta) = (0.2, 1.2)$ works best, under which the tracking results (RTAMSE) are shown in Table 3.

From Table 3, we can see that the value pair of $(\alpha, \beta) = (0.2, 1.2)$ significantly reduces the tracking errors for the drone. This value pair improves the entropy (i.e., the spread) of the likelihood distribution (i.e., the model likelihoods) and almost does not influence the prior distribution (i.e., the prior model weights because $\beta = 1.2 \approx 1$), which means that none of the three models in (53) dominates the rest two models and

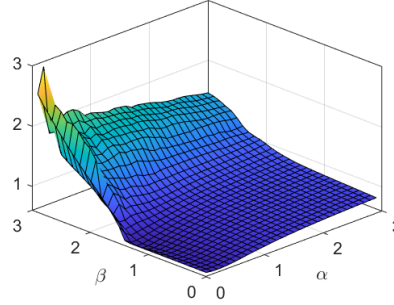


Figure 13: Averaged-RTAMSE performance of the (α, β) -uncertainty-aware IMM filter, against the values of (α, β) . The (α, β) -uncertainty-aware IMM filter with $(\alpha, \beta) = (0.2, 1.2)$ works best.

Table 3: Tracking Results of The Drone: $(\alpha, \beta) = (0.2, 1.2)$

Filter	RTAMSE	Avg Time	Filter	RTAMSE	Avg Time
IMM	0.77	2.71e-05	IMM-UA	0.60	2.85e-05

Avg Time: Average Execution Time at each time step (unit: seconds).

the model set in (53) is not complete (viz., more candidate values for j_k and $a_{j_k, k}$ are expected; only three values are not sufficient).⁴ This implication coincides with our intuition from Fig. 12(b) that, since the drone highly maneuvers with acceleration quickly switching between positive values and negative values, there is no model that dominates the motion of the drone.

Remarks for State Estimation Applications

From our experiments, we found that the grid search method with the step size of 0.01 is an empirical golden rule. As for τ such that $(\alpha, \beta) \in [0, \tau]^2$, experiments suggest that $\tau \leq 3$ is practically sufficient.

⁴For example, $a_{j_k, k} := \{0, -2.5, -5, -7.5, -10, 2.5, 5, 7.5, 10\}$ should be better; however, this introduces much more computational loads in IMM filter. For extensive reading on this point, see Wang (2023, Subsec. VI.A.2.; Tab. III).